NASA Technical Memorandum 104532
AIAA-91-2123

Microanalysis of Extended-Test Xenon Hollow Cathodes

Timothy R. Verhey
Sverdrup Technology, Inc.
Lewis Research Center Group
Brook Park, Ohio

and

Michael J. Patterson
National Aeronautics and Space Administration
Lewis Research Center
Cleveland, Ohio

Prepared for the
27th Joint Propulsion Conference
cosponsored by AIAA, SAE, ASME, and ASEE
Sacramento, California, June 24-27, 1991

NASA

MICROANALYSES OF EXTENDED-TEST XENON HOLLOW CATHODES

Timothy R. Verhey
Sverdrup Technology, Inc.
NASA Lewis Research Group
Brook Park, OH 44142

and

Michael J. Patterson
NASA Lewis Research Center
Cleveland, OH 44135

ABSTRACT

Four hollow cathode electron sources were analyzed via boroscopy, scanning electron microscopy, energy dispersive x-ray analysis, and x-ray diffraction analysis. These techniques were used to develop a preliminary understanding of the chemistry of the devices that arise from contamination due to inadequate feed-system integrity and improper insert activation. Two hollow cathodes were operated in an ion thruster simulator at an emission current of 23.0 A for approximately 500 hrs. The two tests differed in propellant-feed systems, discharge power supplies, and activation procedures. Tungsten deposition and barium tungstate formation on the internal cathode surfaces occurred during the first test, which were believed to result from oxygen contamination of the propellant feed-system. Consequently, the test facility was upgraded to reduce contamination and the test was repeated. The second hollow cathode was found to have experienced significantly less tungsten deposition. A second pair of cathodes examined were the discharge and neutralizer hollow cathodes used in a life-test of a 30-cm ring-cusp ion thruster at a 5.5 kW power level. The cathodes's test history was documented and the post-test microanalyses are described. The most significant change resulting from the life-test was substantial tungsten deposition on the internal cathode surfaces, as well as removal of material from the insert surface. In addition, barium tungstate and molybdate were found on insert surfaces. As a result of the cathode examinations, procedures and approaches have been proposed for improved discharge ignition and cathode longevity.

INTRODUCTION

Operational requirements for electrostatic bombardment ion thrusters place substantial demands on thruster longevity which require long-term operation of hollow cathodes for beam ion production and ion beam neutralization[1,2]. Using mercury propellant, long-life hollow cathode operation at the sought-after operating levels was validated repeatedly[3-5]. With the transition to inert gas propellants and increasing operating power levels demanded from the ion thrusters, new cathode operating conditions are being experienced and previously unobserved problems have arisen.

For the hollow cathode, demands for higher operating power levels have led to higher operating temperatures. Given the temperature-dependent nature of the impregnated insert[6,7], the source of electron emission within the hollow cathode[8], care must be taken not to operate the insert over its recommended temperature if extended life is to be obtained. Typically, this suggested temperature is in the range of 1050-1100 °C[6].

In addition, the use of propellant feed-systems designed for gaseous propellants has introduced the prospect of feed-system contamination that was not a critical issue in the liquid mercury feed systems. There has been an increasing amount of evidence reported in recent years on the destructive effect of feed-system contamination on the hollow cathode. Trace amounts of oxygen and water vapor present in the propellant or evolved from the feed-system are suspected causes of damage to hollow cathodes operated for extended periods. Brophy and Garner[9] reported on the cracking of the hollow cathode tube due to formation of tantalum oxides and the deposition of materials on the inner surface of the insert. Rawlin[10] found the destructive formation of tantalum oxides in the cathode body during operation, leading to its failure. Verhey and MacRae[11] found extensive damage to the internal surfaces of the cathode which included deposition of tungsten and the formation of barium tungstate. Further investigation of that cathode, referred to as WT-I, will be discussed in this paper.

The issues of cathode operating temperatures and propellant feed-system vacuum integrity are critical to understanding the cathode degradation mechanisms and ensuring hollow cathode longevity. Consequently, the primary objective of this effort has been to develop a level of quantitative understanding of the sensitivity of these cathodes and the inserts to oxide-bearing contaminants. The work reported here is the examination of four hollow cathodes operated in different propellant feed-systems to determine the degree of degradation of the insert structure and capability. Two of the hollow cathodes were operated for approximately 500 hours in an ion thruster simulator at a bell jar facility using different operating systems and procedures, but with the same geometrical configuration and under the same conditions. The second set of cathodes is the main discharge cathode and the neutralizer cathode used in an 890-hour life-test of an electrostatic bombardment ion thruster. The results of this life-test with respect to thruster operation and performance have been reported in ref. 12.

Characterization of the respective propellant feed-systems was performed to determine the contamination levels. Microanalyses of the operated cathodes have provided data on the chemistry that occurred during the extended testing. Correlation of the two efforts has led to the development of criteria for propellant feed-system integrity and operation for laboratory- and application-based situations which should reduce the probability of cathode failures due to the suspected causes of oxide contamination.

EXPERIMENTAL APPARATUS AND PROCEDURES

Super Bell Jar 1 Hollow Cathode Wear-tests

The first set of hollow cathodes was operated in a large bell jar vacuum facility, referred to as Super Bell Jar 1 (SBJ1).

SBJ1 Apparatus

Test System The cathode testing assembly and vacuum facility are shown schematically in Fig. 1. The hollow cathodes were mounted in the thruster simulator attached to a diffusion-pumped vacuum chamber which had a pumping capacity of 47,000 l/s which allowed the facility to reach a base pressure of 4.0×10^{-4} Pa. The thruster

simulator consisted of a cylindrical stainless steel spoolpiece which was 30.0 cm deep and 40.0 cm in diameter. In order to simulate the pressure conditions inside a 30-cm diameter ion thruster more closely, a stainless steel screen with a transparency of approximately 20 percent was inserted between the spoolpiece and the bell jar. No magnetic field was incorporated into the simulator.

The cathodes were mounted on a gas plenum chamber. A pressure transducer was mounted on the propellant feed-line on the exterior side of the test flange to monitor the cathode plenum pressure, which was assumed to approximate the pressure within the hollow cathode. The plenum chamber was mounted off the test flange which also supported electrical feedthroughs for heater and ignitor power supplies, thermocouples, and pressure transducers. A quartz window mounted on the side of the simulator was used for a two-color optical pyrometer which monitored the cathode tube temperature. A quadrupole residual gas analyzer (RGA) was also connected to the simulator via a pressure reduction assembly on the RGA which enabled it to monitor the simulator chamber atmosphere at pressures in excess of 10^{-3} Pa.

Hollow Cathodes The cathode geometry tested is shown in Fig. 2. The specifications for all cathodes evaluated in this report are listed in Table I. The dimensions and elements of the cathode inserts are also listed in Table I. Each insert was placed in the downstream of the cathode tube in contact with the interior surface of the orifice plate. Electrical leads from the insert were spot-welded to the inner surface of the cathode tube to provide the electrical connection and to maintain the insert position.

A coiled swaged heater was friction-fitted onto each cathode tube approximately 0.5 cm from the orifice plate (Fig. 2). The heater assembly consisted of a tantalum sheath swaged over a magnesium oxide insulating layer which isolated a tantalum inner conductor. One end of the Ta sheath was closed and the assembly was wound into a helical shape sized to fit on the cathode tube. For the second test, a piece of textured tantalum foil, 45.7 cm long by 2.5 cm wide, was wrapped over the helical portion of the heater. This foil acted as a radiation shield to reduce the heater power losses. The heater was used to raise the temperature of the insert to the surface activation level of approximately 1050 °C. At this temperature, the barium compounds in the impregnate decomposed and free barium migrated to the surface of the insert. The migrating barium lowered the surface work function which lessened the power requirements for discharge maintenance. The heater was positioned to heat the region of the tube containing the insert, while leaving room for a thermocouple to be mounted on the tube. This thermocouple, type R (Pt-13%Rh/Pt), and a two-color optical pyrometer were used to measure cathode temperatures. The thermocouple was spot-welded to the cathode body tube sidewall in front of the heater.

Anode and igniter electrodes The simulator anode was a stainless steel cylindrical shell 15.0 cm long and 19.0 cm in diameter. It was mounted with its midpoint 5.1 cm downstream of the cathode orifice, and was electrically isolated from the cathode and spoolpiece.

For the first wear-test, a stainless steel igniter electrode was positioned 0.32 cm downstream of the cathode orifice. This electrode was a 6.4 cm long by 1.2 cm wide plate mounted on two threaded rods which were parallel to the cathode. An orifice in the center of the electrode allowed the discharge plasma to flow through the electrode. This igniter was removed for the second wear-test as discharge ignition was struck directly between the cathode and the anode liner.

Research grade xenon with a purity of 99.995% was used as the propellant for both tests. Mass flow rates were monitored using electronic mass flowmeters that were calibrated in situ with xenon.

Power Supplies Three power supplies were required to operate the hollow cathode. A 25 volt, 15 amp current-regulated supply operated the cathode heater. A 1200 volt, low-current igniter supply provided the high voltage for the discharge breakdown. A 60 volt, 120 A current-regulated power supply provided the necessary current for maintenance of the discharge after ignition. The cathode and all of the simulator surfaces were maintained at facility ground while the anode was isolated from the spool piece. Examination of the output of the discharge maintenance supply resulted in a substitution of a 400 volt, 50 A supply with a in-house fabricated

current-regulator for use in the second wear-test. This substitution resulted in a significant decrease in ripple in the discharge current, from approximately 50% to 7.4% of the discharge current at the operational set-points. In addition, for the second test, the igniter supply was wired through the discharge supply as the igniter electrode had been eliminated from the thruster simulator.

First propellant feed-system A schematic of the propellant feed-system is shown in Fig. 3. The feed system was fabricated from 11.2 long, 0.46 cm ID 304 stainless steel tubing, except for a 1.0 m long, 0.33 cm ID section of nylon tubing used as a flexible connection to the movable experiment cart. Metal and elastomer compression fittings were used throughout the system. The feed-system had two flow control segments and a vacuum bypass segment. Each flow control segment included an electronic mass flowmeter and a manual flow metering valve. In addition, an orifice bypass segment was installed at the test flange. The bypass segments were installed to speed evacuation of the entire length of the feed-system. Feed-line pressures, upstream of the thruster simulator and cathode, were measured for system evacuation monitoring and leakage rate determination.

Upgraded feed-system The second wear-test propellant feed system was upgraded with the following changes: shortened the overall line length to 7.4 m; used 0.77 cm ID tubing for 4.0 m of the feed-system; eliminated nylon tubing; and used vacuum-type fittings throughout, except where precluded by a device-dependent fitting type. The system remained broken down into two flow control segments, each of which included a manual metering valve for flow control and an electronic mass flowmeter for flow monitoring. There was a vacuum bypass segment in the flow control portion of the feed-system and an orifice bypass at the test flange.

Cathode testing procedures

Cathode activation and ignition procedures Insert activation procedures were used to prepare the cathode insert for emission by driving off contaminants from the surfaces of the insert and cathode, thereby decreasing the probability of destructive surface reactions via oxidation. In addition to removing oxides, the procedures resulted in barium being brought to the insert surface which led to easier starting of the discharge and lower power consumption during discharge operation. Different activation procedures were used for the two tests. The first procedure consisted of the following steps. The feed-lines and cathode were first purged with xenon gas at a flow rate of 27.0 sccm for 20 minutes. Following this, the swaged heater was started at 1.0 A and the applied current was raised in 2.0 A increments at 15 minute intervals to a maximum power of approximately 90.0 W. At this point, the temperature of the cathode body was approximately 800 °C. The cathode discharge was started by pre-setting the discharge supply to 10.0 A and increasing the output voltage of the igniter supply, applied between the cathode and the igniter electrode, until electrical breakdown to the anode liner occurred. After ignition, the heater power and igniter supplies were shut off, the propellant flow was decreased, and the discharge current adjusted to the desired levels.

For the activation procedure of the second wear-test, derived from the Solar Electric Propulsion System (SEPS) development program[13], the cathode and feed-lines were again purged with xenon for 20 minutes, but at a 10.0 sccm flow rate. The swaged heater was turned on and set to an input power of 18.0 W which resulted in a cathode tube temperature of 500 °C. The cathode was maintained at this temperature for 3.0 hours. The heater power then was shut off and the cathode was allowed to cool for 0.5 hours. The heater power was applied again, but this time at a power level which yielded a cathode tube temperature of 1050 °C, typically 95-100 W. The cathode was maintained there for 1.0 hour. After the high-heat stage, the heater was shut off for at least 0.5 hours. This activation procedure was used each time the hollow cathode was exposed to atmosphere. If the cathode had been under vacuum continuously, then only the ignition procedure was required to light the discharge. For discharge ignition, xenon gas was purged through the cathode for 20 minutes. Heater power was then applied to bring the cathode temperature up to 1050 °C. After the cathode was maintained at this temperature for at least 0.5 hours, the discharge supply, with an open-circuit voltage of approximately 100 V between cathode and anode, was turned on. If greater

voltage was needed for discharge ignition, the igniter supply was also turned on and the voltage raised until electrical breakdown occurred. Once ignited, the heater and igniter supplies were shut off and the xenon flow rate and discharge operating current were adjusted to the desired levels.

Cathode operating points Both cathode tests were conducted at the same conditions which were chosen to correspond to the operating point for the main discharge cathode of a 5.0 kW ion thruster. The cathodes were operated for the test at a discharge current of 23.0 A and a xenon mass flow rate of 6.1 sccm. The discharge voltage and cathode tube temperature were consequences of these set points and the electrode configuration. All of the operating parameters are listed in Table II.

Summary of WT-II test results

The operating parameters of the first wear-test (WT-I) were discussed in ref. 11 and are summarized here in Table II. The bulk of the test description presented here will therefore focus on the second wear-test, with comparisons to the first test being made later in the paper.

Prior to beginning the test, the hollow cathode was operated for 41 hours at various xenon flow rates from 3.0 to 10.0 sccm and emission currents between 5.0 and 28.0 A. The wear-test itself lasted for 478 hours and was performed over three segments due to two system shut-downs. The first, at hour 332, was a facility shut-down due to power failure and the second was an intentional shut-down of discharge operation at hour 428. These shut-downs did not significantly alter the operating parameters of the test.

Prior to and after the test, the current-voltage characteristic curves of the cathode were obtained. After test initiation, the discharge voltages at all currents decreased, but were quite consistent throughout the remainder of the wear-test (see Fig. 4). Data sets 1 and 2 were taken just prior to completion of test segments 2 and 3, and set 3 was taken after the wear-test had been completed and the cathode was reactivated after being exposed to atmosphere for several days. One possibility for the initial change in characteristic behavior may have been the result of further conditioning of the cathode by discharge operation.

A primary parameter of interest was the cathode body temperature. Figure 5 shows the plot of the cathode temperature over the course of the test as measured by the thermocouple. The temperature was found to be stable for most of the test, after it had decreased from a maximum of 1146 °C at start-up to an average level of 1100 °C. The test shut-downs did not cause a significant change in the operating temperature as measured by the thermocouple and the optical pyrometer measurements confirmed these results qualitatively. Further discussion of temperature behavior will be presented in the next section.

The discharge voltage level over the course of the test is plotted in Fig. 6. The voltage decreased continually from 23.0 to 19.0 volts during the first segment of the test. After the first shut-down, the voltage stabilized at approximately 18.0 volts for the remainder of the test. The voltage behavior was consistent with changes in the cathode tube temperature. The levels of irregular ripple in the discharge voltage and current were found to be 14.7% and 7.4% (±1%) of the output values and remained relatively constant throughout the wear-test. However, the impact of ripple on cathode condition, if any, is not known at this time.

In addition to the operating voltage, the starting voltage of the discharge was also monitored. For all starts, the discharge was ignited with 100 volts or less, thus the igniter supply was not needed for any of the starts during the test. For the last two starts, one of which was performed after the cathode had been exposed to atmosphere for several days, then reactivated using the prescribed procedure, the breakdown voltages were 25.0 and 22.0 volts respectively.

Over the course of the wear-test, the measured orifice diameter of 0.14 cm (±0.004 cm) did not change in size. The resulting emission parameter (emission current/orifice diameter) was 16.0 A/mm. This orifice size also resulted in a constant internal cathode pressure of approximately 7.9×10^2 Pa over the course of the test.

The levels of contaminants were monitored continuously via the RGA during the first segment of the test. The partial pressures of air and water vapor started out at approximately 1.3×10^{-3} and 8.6×10^{-4} Pa respectively. The air level reached a maximum of 3.9×10^{-3} Pa 25 hours into the test, then

decreased to the detection limit of the RGA at approximately 1.1×10^{-4} Pa by hour 300. The water vapor level peaked at about 2.5×10^{-3} Pa within the first hour of testing, then decreased to the RGA detection limit within the first 80 hours. The maximum partial pressures of the contaminants represented approximately 8.7% and 5.7% of the total operating pressure of 6.0×10^{-3} Pa within the thruster simulator chamber. The described behavior was indicative of material outgassing from the test hardware at the elevated temperatures. It should be noted that four factors must be considered when interpreting the RGA results. First, it was assumed that the readings obtained from the thruster simulator by the RGA reflected equivalent conditions inside the hollow cathode. Second, the RGA sensitivity used to determine pressure levels was assumed to be constant for the AMU range of 18 to 32, as the measured sensitivity of N_2 was used for air and water vapor values. Third, the measured sensitivities were taken with a second quadrupole head installed in the RGA and correlated to the respective N_2 levels by using the Argon sensitivity to interpolate between the two heads. Finally, no correction for mass dependence of gas arriving at the quadrupole head within the RGA as a result of the differential pumping was undertaken. It was assumed that the RGA sensitivity was constant over the mass range of 18 to 40 AMU. The RGA was damaged during the first shutdown and was not available for the remainder of the test.

Comparison between wear-tests The operational parameters exhibited many differences between the two wear-tests. Compared in Fig. 6 are the discharge voltages of the two cathodes over the course of the tests. In the first wear-test, voltage rose irregularly from 15.0 to 21.0 volts, with most of the rise occurring after the facility shut-down at hour 195. During the second test, the discharge voltage dropped from 22.5 to 18.0 volts. The decrease in voltage was linear throughout the first test segment, but remained stable there after. As has been mentioned previously, the decrease in voltage may be attributable to continued conditioning of the insert by the discharge. There were several possibilities which might account for the rise in discharge voltage in cathode WT-I including degradation of the insert emission capability and deposition of material on the anode surfaces causing an increase in surface resistivity. The former possibility was substantiated by the increasing difficulty in discharge ignition and the later by the presence of a coating on the surface of the anode at the completion of the first wear-test.

The current-voltage characteristics of the two tests can be compared between Fig. 4 and Fig. 7. The discharge voltage ranges were similar with the first test having a lower limit of 15.0 V. However, the rise in voltage at the higher currents that was experienced in the first test never occurred for the second cathode WT-II. Also, the post-test voltages were lower for cathode WT-II, while the opposite occurred for the first wear-test.

The starting characteristics of cathode WT-II showed substantial improvement over those of cathode WT-I. For all starts of cathode WT-I, the xenon mass flow rate needed to be raised to 30.0 sccm or greater and the igniter power supply turned up to several hundred volts before ignition would occur. But, for cathode WT-II, the flow rate was never raised above 10.0 sccm and the applied voltage never exceeded 80.0 volts to obtain discharge ignition throughout the wear-test.

The cathode temperatures over the course of the test also differed in behavior, as can be seen by comparing the curves in Fig. 5. The temperature rose throughout the first test to reach a maximum of 1210 °C at the end of the test. Note that the rise in cathode temperature became regular and continuous after the first shut-down. For cathode WT-II, the temperature started at a maximum value of 1146 °C and decreased to an average value of 1100 °C. The cathode temperature showed a small rise upon restart after the first shut-down, but that quickly decayed to the steady-state value. Similar behavior was observed at the beginning of the third test segment.

Cathodes WT-I and WT-II temperatures both increased with emission current, as can be seen in Fig. 8. However, cathode WT-I experienced higher temperatures over most of the current range, particularly at 5.0 A, where cathode WT-II operated approximately 200 degrees lower than cathode WT-I. This difference decreased to about 50 degrees at 25.0 A.

Ring-cusp Ion Thruster Life-test

A 890-hour life-test was performed during December of 1989 and January of 1990 in order to test the extended operation capabilities of a ring-cusp ion thruster operating at 5.5 kW. The examination of the main discharge and neutralizer cathode are reported in this paper in order to compare the condition of these cathodes with those tested in the SBJ1 facilities.

Thruster Apparatus

Test system The two hollow cathodes used in the thruster were the main discharge cathode and the neutralizer cathode. The main discharge cathode, referred to as TL-I, was identical in geometry to the two SBJ1 wear-test cathodes as can be seen in Table I. The neutralizer hollow cathode, designated TL-II, was shorter and had a smaller orifice, but otherwise was identical to the other cathodes. Each cathode had a swaged heater identical to the ones used in the SBJ1 tests friction-fitted onto the ends. Further details on thruster operation and performance are available in ref. 12. The discussion here will be limited to description of the propellant feed-system and its characterization.

Propellant feed-system The thruster had three separate propellant inputs: main cathode feed, main plenum feed, and neutralizer cathode feed. The feed-system is shown schematically in Fig. 9. All three lines had the same source for the xenon propellant gas (research grade purity, 99.995%) and the argon purge gas (research grade purity, 99.995%). After the gas input, the lines were separated into three flow control segments. Each segment consisted of a manually-operated metering valve and an electronic mass flowmeter. The propellant feed-system between the xenon bottle and the vacuum flange was fabricated from 0.46 cm ID 304 stainless steel tubing, with either A-N or elastomer compression fittings for assembly. On the interior side of the vacuum flange, the gas lines were made of 0.60 cm dia. Viton tubing with a 0.33 cm inner diameter to enable a flexible connection between the vacuum flange and thruster. The Viton hoses were connected to steel adaptor tubes that were attached to the cathodes and main feed plenum. The overall lengths of the cathode lines were 5.2 m for the main discharge and 5.1 m for the neutralizer cathode. The main plenum feed-line was approximately 5.2 m in length.

Thruster operation

Cathode activation and ignition procedures The cathode activation procedure used for conditioning both the main and neutralizer cathodes was the same as the procedure used for cathode WT-I. The ignition procedure for cathode TL-I was identical to that of cathode WT-I, except for discharge ignition. For the thruster, a 3.0 kV pulser instead of a high voltage supply was used to light the discharge. For the neutralizer cathode which had a keeper as part of its design, a keeper voltage of approximately 380 volts was applied to the cathode three-quarters of the way into the pre-heating stage of the activation (45 min.). The keeper discharge typically lit at this application and drew a current of 2.5 A. Once the beam was formed, additional current was drawn from the neutralizer cathode to match the beam current.

Cathodes operating parameters The thruster life-test was operated at the 5.5 kW total processed power which corresponded to an emission current of 18.8 A and average cathode-to-anode voltage of 26.9 volts for cathode TL-I and an emission current of 6.0 A and neutralizer-to-ground voltage of 15.4 volts for cathode TL-II. Propellant flow rates were initially 4.0 and 3.3 sccm of xenon for cathodes TL-I and TL-II, respectively. No cathode temperatures were measured during the test, but, using results from parametric testing of cathodes at SBJ1, the cathode TL-I geometry was estimated to have a tube temperature of approximately 1150 °C. No temperature data existed for the neutralizer geometry.

History of thruster operation Prior to the life-test, the thruster was operated for 65.4 hours, 16.0 hours at the 5.0 kW level and the remaining 49.4 hours at various throttled conditions, for system check-out. A summary of the cathodes operational parameters is provided in Table III. Over the course of the test, cathode TL-I propellant flow-rate rose from 4.0 sccm to 4.6 sccm in order to maintain constant discharge voltage. Neutralizer operation was altered during the first 300 hours of the test. First, the keeper discharge power supply was modified in order to

maintain discharge stability. Secondly, xenon flow was raised from 3.3 to 5.2 sccm over the course of the life-test to mitigate increasing beam coupling voltage and to stabilize the keeper discharge.

The life-test lasted for 890 hours during which the thruster experienced 7 discharge shut-downs. The restarting condition and requirements are listed in Table III. After change-out of the xenon gas supply at hour 890, cathode TL-I restarted with no problems after reactivation, but cathode TL-II experienced faulty power supply operation which resulting in destruction of the keeper electrode and operation in a high-voltage mode. The test was subsequently terminated.

The usefulness of the condition of the neutralizer cathode, TL-II, as an accurate measure of cathode longevity was limited by the inadvertent operation of the neutralizer in the off-normal conditions listed above. Consequently, the neutralizer condition was documented for comparison purposes only and should not be taken as indicative of the end condition of a properly operated neutralizer.

Propellant feed-systems characterization

All three propellant-feed systems were examined to determine contamination leakage levels. For quantifying leak-rates, the primary technique employed was to evacuate the feed-system to a desired vacuum level ($<10^{-2}$ Pa), after which the system was isolated. Pressure gauges mounted in the feed-system were then monitored to determine changes in internal pressure as a function of time. Figure 10 shows the plot of the in-line pressure as a function of time for both of the SBJ1 propellant-feed systems and the thruster cathode feed-lines. The rapid rise in the first portion of the curves represented the contribution for outgassing[14]. This contribution has been calculated to be substantial for the feed-system designs used here, but it would decay exponential with time and was expected to reach a negligible level within a time-span that was short compared to the extended test length. Consequently, the later portions of the curves represented the leakage rates that were present over the course of the test and, as such, were used to compare the four feed-systems. For the SBJ1 systems, the leakage rates were determined to be 3.7×10^{-4} sccm and 6.4×10^{-5} sccm for the cathodes WT-I and WT-II, respectively. The upgrades to the facility resulted in a 140% decrease in measured leakage rate, as well as the apparent elimination of the outgassing contribution, relative to the other systems. For the thruster cathodes TL-I and TL-II, the leak rates were found to be 2.9×10^{-4} sccm and 2.7×10^{-4} sccm, respectively. The leak rates of the thruster lines were in agreement between themselves, with a difference of 7%, but were, on average, 27% less than the WT-I feed-system and 125% greater than the WT-II system.

In addition to the above technique for leak-rate determination, another method was employed. A helium leak detector was used to measure leak-rates as a means of validating the earlier results and to separate the different contributions of physical leakage and outgassing form internal surfaces. The results of the leak detector were the values $\geq 10^{-7}$ sccm and 1.7×10^{-7} sccm for the first and second wear-test feed-systems, respectively. Further work on leak-rate determination is needed to assess the difference in leakage rates as estimated by the two techniques. The reason for the limit value for the first wear-test system rather than a single value resulted from the fact that the layout of the feed-system prevented enclosure which was required for quantitative helium leak detection. The design of the later system enabled it to be enclosed and quantitative helium leakage rates obtained. Helium leak tests of the thruster feed-system were not undertaken because it was also not enclosable.

The leakage determined for all the systems represented contaminant levels that, at xenon flow rates of approximately 5 sccm, would be between 10 and 100 parts per million. Given the specified purity level of approximately 1.0 ppm for the supplied xenon propellant, it was felt that the propellant would pick up the largest part of its contamination from the feed-system. Consequently, the impact of initial propellant gas impurities (before exposure to propellant feed-system) on cathode longevity was felt to be secondary within the test systems reported, but may become an issue in future tests.

With the upgrading of the propellant feed-system for cathode WT-II, there was a significant improvement in the cleanliness of the system due to the reduction in feed-line leakage. This

improvement was attributed to changes in feed-system design and assembly which will be discussed in the criteria section.

EXAMINATION OF HOLLOW CATHODES

Sample Preparation

Preparation was required to examine the cathodes with the techniques used. For the boroscope examination, the cathode tubes were cut down to a length of approximately 4.4 cm long in order to accommodate the microprobe used for internal surface examination. The cathodes were sliced longitudinally with a diamond saw to lengths of between 2.2 and 2.8 cm to expose the internal surfaces for scanning electron microscopy (SEM), energy dispersive x-ray analysis (EDS), and x-ray diffraction analysis (XRD). The cutting of the cathodes were done using kerosene as a cutting fluid or with no cutting fluid to minimize interactions with the impregnate. It was found that much of the deposited structures observed on the orifice plate and insert surfaces with the boroscope were removed by the slicing. Whenever possible, this material was collected and analyzed for elemental and molecular composition.

Photo-documentation

The external surface conditions of the cathodes were examined prior to and after all the tests. For the first wear-test, cathode WT-I had not previously been used. The orifice plate showed machining marks and the electron-beam weld was clearly visible, as shown in the photograph in Figure 11(a). In addition, the edges of the chamfer were well-defined and the chamfer had the same smoothness as the plate surface. After the wear-test, the orifice plate was substantially roughened over its entire area, including the chamfer (Fig. 11(b)). The Ta foil thermocouple cover junction appeared severely eroded and heat-treated. Also, the downstream end of the cathode body tube had the appearance of being eroded up to the point of coverage by the swaged heater.

The initial condition of cathode WT-II shows in Fig. 12(a) the effects of 41 hours of discharge operation prior to the wear-test. The orifice plate was already eroded and exhibited the roughened appearance on plate, chamfer, and e-beam weld surfaces. However, the orifice geometry had not been altered; the chamfer was straight and the orifice had the specified size and shape. The Ta foil cover over the thermocouple junction was undamaged. Post-test examination of the condition of the orifice plate showed no discernible change (see Fig. 12(b)). The cathode tube exhibited the same surface erosion observed on cathode WT-I and the Ta foil was sufficiently embrittled to flake off when a slight force was applied.

Prior to the life-test and the initial check-out period, both cathodes TL-I and TL-II were in pristine condition, as shown in Fig. 13(a) and 14(a). Post-test examination showed several changes which are shown in Fig. 13(b) and Fig. 14(b). Cathode TL-I experienced severe ion bombardment of the orifice and orifice plate. The surface had been roughened to the point of removing all pre-test features including the electron-beam weld structure. The chamfer on the orifice appeared to no longer be a smooth 45°, but very irregular and filled-in. In addition, the orifice, while not changing significantly in diameter, had an irregular geometry with one edge being opened up, possibly by erosion. There also appeared to be irregular metallic deposits on the orifice plate.

For the neutralizer cathode TL-II, the orifice plate had been roughened, but not as severely as cathode TL-I. There were regions on the orifice plate where the original machining marks were still visible and the electron-beam weld structure was visible over the entire surface. However, the orifice shape was irregular and material was deposited in the chamfer and channel regions.

Inside cathode WT-I, the shape of the orifice chamfer and channel appeared intact. However, a large deposit of material was found at the downstream end of the insert and on the orifice plate, as shown in Fig. 15(a). The rest of the insert surface was divided up into three regions with decreasing degrees of roughness and different colors. The insert surface was slightly irregular, indicating material removal. There was also material visible between the insert outer wall and cathode body tube. This material may have been responsible for affixing the insert to the cathode body.

The inside of cathode WT-II is shown in Fig. 15(b). There appeared to be material deposited on the orifice plate

and at the downstream end of the insert. The remainder of the insert surface was separated into different colored regions, all with approximately the same degree of roughness. The insert surface has one distinct boundary at approximately 0.85 cm from the orifice plate and another, less distinct, boundary at 1.6 cm. The insert wall thickness was uniform and the surface was smooth. The orifice chamfer and channel appeared to be in near original condition with no deposition visible.

The interior surface of cathode TL-I is shown in the photograph in Fig. 16(a). While the orifice channel was open, the chamfer has been filled in and that the deposited material extended into the cavity. The insert wall was tapered by tungsten removal which was most severe at the downstream end and appeared to decrease linearly with distance from the orifice plate. Several different regions of the insert were distinguished by coloration and degrees of roughness. A large portion of the gap between insert outer wall and cathode body tube was apparently filled in at different points.

The sliced cathode TL-II is shown in Fig. 16(b). As previously indicated, the orifice was closed down and altered in shape by material deposition. Material also appeared to be deposited on the upstream side of the orifice plate. The insert surface was not altered as substantially as that of the main cathode. Removal of the tungsten was limited to the downstream end of the insert, where thinning of the wall was visible. Deposits of material were visible at this end of the insert. A large chunk of material broke off the cathode during slicing and was suspected of fitting into the downstream end. The rest of the insert surface was divided into distinct regions, the largest of which extended over approximately two-thirds of the surface at the upstream end. Parts of the gap between insert and cathode tube were filled with material, primarily in the downstream end of the cathode. The ring visible at the upstream end of the insert was a portion of the molybdenum collar.

Boroscope examination

All cathodes, except for WT-I, were examined with a boroscope in order to inspect the internal surface features before the cathodes were sliced to document the conditions which were altered by the cutting process. The boroscope's fiber-optic probes, inserted from the upstream end of the cathode tube, provided visual access. In order to provide a guide for the reader, cross-sectional schematics of the examined hollow cathodes have been devised in Figures 17 through 20, which qualitatively present the observed features on the insert surfaces. Also indicated by figure number in these diagrams are the locations of SEM photographs. Finally, the various regions described in the SEM and XRD examinations and their elemental compositions are indicated with the bars at the diagram bottom. Figure 17 is for cathode WT-I, for which the boroscope was not available.

For cathode WT-II, the orifice plate and insert surfaces were observed to be in relatively good condition. The orifice appeared to be surrounded by a rough ring of deposited material, but it was difficult to distinguish the amount. Outside of this ring, some material had collected over the rest of the orifice plate in grain-like structures. The downstream end of the insert had a ring of crystal growths that stuck fiber-like out from the surface, as indicated in Fig. 18. These fibers appeared to be deposited metal and have very reflective surfaces. The ring was very narrow and had a distinct boundary with a region of very fine structure. This next region appeared to be uniformly covered with fibrous crystals, possibly of similar composition as the larger growths observed at the insert edge. Upstream of the fibrous growth, the remainder of the insert surface appeared uniform and without any distinct features, though different color striations were apparent. The molybdenum collar at the upstream insert end appeared clear of material deposition. Crystal growth was apparent in the gap between insert wall and cathode tube wall with some material extending further upstream of the moly collar. Later boroscope examination did not find this material as it was lost when the insert was found to be removable.

In cathode TL-I, the orifice appeared to be free of obstruction. Around the orifice, material was deposited non-uniformly. There also appeared to be a notched area in the orifice, approximately 0.05 cm wide by 0.02 cm deep, which corresponded to the slightly opened area observed in the photograph of the orifice plate. A short distance upstream of the orifice

plate on the insert (see Fig. 19), a large ridge-like deposition of material that covered the entire circumference of the insert was observed. There was a notch in this ridge that corresponded to the notch observed in the orifice plate. Another ridge of material was observed upstream of this first deposition. Moving further upstream, the surface growth became fiber-like, though the density of coverage remained high. This region of crystal fiber growth had a distinct upstream boundary where the insert surface changed to a more uniform surface, with none of the large material formations seen near the orifice plate. The growth appeared much finer and closer to the surface. There was also a larger irregular structure on the surface which seemed to break up the surface. A distinct, but irregular boundary defined the far edge of this region. At the upstream end of the insert, there were few crystal growths visible, though the surface had a roughen appearance. As was found in cathode WT-I, the gap between insert and tube wall was found to be filled with a crystal growth formation. The crystal growth extended upstream of the gap along the wall of the tube. The molybdenum collar on the insert had material deposited in large grain structures on the surface perpendicular to the tube wall. In addition, material collected in smaller formations on the collar surface parallel to the tube wall.

The interior of cathode TL-II is represented in Fig. 20 and had many of the same characteristics as cathode TL-II. The orifice was found to be blocked (visually) by a large metallic deposit. The material of this plug extended into the insert cavity as well as covered a substantial area of the orifice plate. However, the degree of physical blockage was unknown. The downstream insert surface area possessed several ridge-like features which were relatively symmetric. The entire length of the insert surface seemed to be covered with fibrous crystal growth which covered the surface very densely and extended into the insert cavity. The farther the distance upstream from the orifice, the less apparent the growth appeared, until the insert surface had a smooth appearance. However, at the upstream end of insert, the crystal formations increased in density symmetrically over the surface. Material was deposited on the surface of molybdenum collar parallel to the tube wall. There was a extensive formation of fibrous crystals that occurred between the insert and the cathode tube wall. This formation extended up from the gap between insert and tube wall along the electrical lead length.

Dental Impressions

Dental putty impressions of the post-test condition of cathode WT-II and the pre- and post-test conditions of the thruster life-test cathodes examined via a shadowgraph. For WT-II, the impression revealed that the orifice diameter and the angle of the chamfer had not changed from the fabrication specifications over the course of the wear-test. For cathode TL-II, the impression verified that the 45° chamfer on the downstream side of the orifice has been eliminated, apparently filled in by material deposition. However, the diameter of the orifice had not changed size greatly, closing down from 0.15 cm to 0.14 cm. The impression confirmed that the orifice of cathode TL-II had been plugged during the life-test.

SEM examination

All cathodes and inserts were investigated by secondary electron spectroscopy to resolve physical features, backscattered electron spectroscopy to distinguish between materials on the surfaces, and energy dispersive x-ray analysis which was able to determine elemental composition. The cathodes were surveyed to determine the type and extent of life-limiting damage that occurred. Figures 17-20 have the locations of the described SEM photographs indicated.

In cathode WT-I, the most prominent change found was material deposition, which occurred primarily in the downstream end of the cathode. The channel and chamfer of the orifice were clear of any obstruction, though the surface appeared to have some amount of deposition on it, as can be seen in the photograph in Fig. 21. There was a substantial tungsten deposition on the upstream side of the orifice. The deposition was roughly uniform around the orifice and had a diameter of approximately 2.8 mm.

The insert deposition on cathode WT-I was also found to be tungsten with a structure that was roughly filamentary and showed no crystalline-like behavior

(Fig. 22). The deposition appeared to be uniform over the surface in this region. The insert surface upstream of the tungsten deposition was roughened and experienced substantial material removal which had left it more porous than before use. Moving further upstream, sharp-edged crystalline formations of tungsten appeared among the smoother shapes of the sintered tungsten grains, as shown in the photograph in Fig. 23. The photograph shows the surface material under secondary electron (SE) illumination on the left side and backscattered electron (BSE) illumination on the right. At this distance from the orifice, material composed of tungsten, barium, calcium, and oxygen was found to have formed in the gap between the insert outer wall and the cathode tube wall. The probable source was migration of impregnate from the insert pores, affixing the insert into the cathode tube.

Approximately 0.65 cm from the orifice plate, an amorphous substance formed among the tungsten grains. EDS identified the material as a compound containing tungsten, barium, calcium, and oxygen, and was probably an oxide. Some areas of the surface charged under secondary electron emission, which indicated that these areas were nonconductive. The area covered by this material increased further from the orifice plate and reached a maximum coverage at a distance of approximately 1.3 cm from the orifice where it covered most of the insert surface, as shown in Fig. 24. The BSE image indicated that the surface layer was uniform in composition with small grain-like tungsten structures on its surface. The coverage of the surface decreased quickly further upstream. The insert surface took on a grainier appearance, with grain sizes ranging from 3 to 5 microns (region 3, Fig. 17). The insert surface had lost the machine-smeared grain appearance of an unused insert, probably due to removal of the tungsten surface layers, which exposed the bulk tungsten grains. EDS examination showed only the presence of tungsten, with trace amounts of molybdenum, and aluminum. The molybdenum must have come from the molybdenum collar or the cathode body tube.

Cathode WT-II was found to have several differences in condition with the first wear-test cathode. The photograph in Fig. 25 shows the cathode orifice and the downstream region of the cathode. The orifice channel and chamfer were in very good condition, showing no signs of change in size or shape. The surface of the orifice channel appeared similar to that of cathode WT-I, though the apparent deposition was not as heavy. Small amounts of barium and calcium were also found in the channel. Material deposition occurred in the area surrounding the orifice which looked similar to the deposition formation around the orifice of cathode WT-I, though not nearly as substantial. It formed a ring around the orifice with an inner diameter of approximately 1.9 mm and an outer diameter of 2.3 mm. EDS determined that it was tungsten metal with a trace amount of barium. The cathode tube wall and the insert were examined separately since the insert was removable. In Fig. 26, the photograph shows where the insert had been by the presence of material collected on the tube wall. This material was composed of barium, calcium, tungsten, oxygen, and aluminum with trace amounts of molybdenum and rhenium. The relative amounts of the elements in this compound were found to vary with location and surface geometry.

The insert surface condition was also found to be position dependent, with three distinct regions (see Fig. 18). The photograph in Fig. 27 shows the surface of the first region at the downstream end of the insert which had the structure of the sintered tungsten. Only tungsten was found in this region, indicating that all barium and its compounds had been removed from the surface during discharge operation. The second region, approximately 1.2 cm from the orifice plate, consisted of a darker band on the surface that was approximately 1.1 mm wide. The gray shading of the grains in the BSE image in Fig. 28 was a surface coating composed of tungsten, barium, calcium, oxygen, and trace amounts of aluminum and molybdenum. The white grains on top of the coating were tungsten. In the third region of the insert, the surface was also found to have a coating, though not as uniform as the second region, and which had much more material collected on top (Fig. 29). The coating, distinguished in the BSE image by the darker color, was composed of tungsten, barium, and trace amounts of calcium, aluminum and molybdenum, and was very similar to that of the second region though the signals for all elements other than tungsten were weaker. Oxygen was assumed to be part of this material. At the upstream end

of the insert, the surface coating was still present, but molybdenum amount had increased and rhenium was found by EDS, suggesting removal of material from the cathode body tube or electrical leads.

The orifice of cathode TL-I is shown in the photograph in Fig. 30, which confirmed that the chamfer was filled in and that material was deposited along the entire channel. The deposition extended the orifice channel into the cathode by approximately 0.2 mm. EDS determined that the deposited material was tungsten metal. In addition, deposition also occurred on the outer surface of the orifice plate, as indicated by the slight rises on the orifice plate surface. The photograph in Fig. 31 shows that the inner surface of the orifice plate was roughened severely by discharge operation, probably due to removal of the thoriated tungsten and deposition of insert material removed from the upstream surface. The roughness increased with distance from the orifice. At the outer edge of the visible range of the plate, there were large formations of deposited materials which had a crystalline appearance. Material composed of barium, aluminum, tungsten and oxygen, which was probably an oxide, was also found deposited on the orifice plate. This compound is distinguished in the BSE photograph in Fig. 32 as the darker material that seemed to be coating the tungsten formations. Distribution of the compound peaked midway between the orifice and the cathode insert, with coverage being lightest near the orifice plate. The lighter areas in the photo were composed primarily of tungsten, with trace amounts of barium, aluminum, and molybdenum.

Three distinct regions were found on the insert surface as indicated in Fig. 19. Fig. 33 shows a photograph of the insert surface near the orifice plate. This first region exhibited the sintered grain structure of the tungsten matrix material and the BSE image shows that the surface was roughly homogeneous. EDS verified that tungsten was the primary element in this area, with only trace amounts of barium. This region gave way to a rougher surface which is shown in the photograph in Fig. 34. The surface was more porous with a large amount of barium compound among the grains, which was composed of tungsten, barium, and probably oxygen and was the darker material in the BSE image. The presence of the barium compound decreased and the occurrence of larger, crystalline grains increased further upstream, which peaked at approximately 0.65 to 1.3 cm from the orifice plate. The deposited structures observed by the boroscope that had been removed by the slicing process probably came from this region. These tungsten deposits were examined separately with the SEM and were found to have a crystalline formation, as can be seen in the photograph in Fig. 35. The presence of the crystalline structures decreased further upstream.

Fig. 36 shows a photograph of the surface of the third insert region. Large layer formations, which were composed of tungsten, barium, and oxygen with trace amounts of molybdenum, aluminum, and rhenium, covered the surface. Charging of the surface during examination indicated that it was nonconductive. The composition and behavior was similar to analogous layer structures seen in the SBJ1 wear-test cathodes and, as such, was assumed to be an oxide. The coverage of the surface material was nearly complete at the upstream end and small tungsten structures were scattered on top of the layer.

The gap between insert outer wall and cathode body tube was open except for some material that had been moved into it by the slicing process. However, the insert was affixed in the cathode body tube as had happened in cathode WT-I.

For the neutralizer cathode TL-II, the internal surface conditions were similar to cathode TL-I, with some differences. Fig. 37 shows a photograph of the orifice region. The chamfer and channel were substantially altered and showed deposition of material over both surfaces in a rough, grainy layer. The deposited material, which was determined by EDS to be tungsten, did not have the solid appearance of the orifices in the rest of the cathodes. The upstream side of the orifice plate suffered extensive damage and deposition of material. The entire inner surface was covered with deposited material as shown in the photograph in Fig. 38. The larger structures in the photograph were crystalline formations of tungsten metal. Compounds which were suspected of containing barium were found on this surface, among the tungsten formations, as indicated by the gray areas in Fig. 39.

The formation and composition of deposited structures on the downstream end of the insert were similar to those on the orifice plate. The surface of

the region immediately next to the orifice was extremely rough, as can be seen in Fig. 40. The BSE image shows that the surface material was relatively homogeneous and EDS determined it to be tungsten. This region extended approximately 0.3 cm upstream of the orifice and was probably the region where the chunk of tungsten, formed as a cap over the orifice, was located inside the insert. This plug had a diameter of approximately 3.2 mm and is shown in Fig. 41.

The remaining area of the insert surface was divided up into two regions (see Fig. 20). Upstream of the crystalline formations, the surface was composed of rough granular structures which were found to be primarily tungsten, with trace amounts of barium and aluminum (Fig. 42). In this region of the insert, a nonconductive material was found to have filled the insert-cathode tube gap; probably formed from impregnate migrating out of the insert pores. This material may account for affixing the insert in the cathode tube, like cathodes WT-I and TL-I. The white appearance of the material in the image on the left of Fig. 43 indicated that the material was charging. EDS determined that the material was composed of tungsten, barium, oxygen, and trace amounts of calcium, molybdenum, and aluminum. The BSE image shows the gap material as darker than the wall materials, which indicated that the compound was probably an oxide.

The final region of the insert surface was covered with a uniform layer, composed of tungsten, barium, calcium, and oxygen. The photograph in Fig. 44 shows the boundary where the surface coating began. It was very homogeneous under BSE and was similar to other layer formations observed on the other inserts. On top of this layer, small tungsten structures were found scattered. The nonconductive portions of this layer were not symmetric over the insert surface and neighboring regions of the layer did not charge under secondary electron emission even though they were composed of similar material. These layer structures were present to the end of the insert, but different elements were included in its composition. The tungsten grains on the surface became more numerous away from the boundary. Near the upstream end of the insert, the primary elements were molybdenum, rhenium, and small amounts of tungsten, barium, oxygen, and calcium. The composition changed again in the region next to the molybdenum collar at the end of the insert. Here, the primary element was rhenium, with small amounts of barium, tungsten, oxygen, and molybdenum. A uniform layer of material was found on the molybdenum insert collar. This layer was composed primarily of rhenium, with a small amount of molybdenum and trace amounts of barium and aluminum. The rhenium must have come from the cathode body tube or the electrical leads.

X-ray Diffraction examination

X-ray diffraction (XRD) analysis was performed on films of sample material lifted from the surfaces. The insert of cathode WT-I was examined in three regions, as indicated in Fig. 17. The first region showed only tungsten, with unidentifiable trace compounds, in agreement with the EDS analysis which determined that the deposited material was pure metal rather than an oxide. The second region was found to contain mono-barium tungstate, $BaWO_4$, in addition to tungsten. There may have been trace amounts of di-barium tungstate, but the signal was very weak. The third region did not yield a clear signal as to composition of the surface material; the signal that was obtained showed a unidentifiable tungsten compound. This lack of a signal indicated that the surface material, readily visible by SEM, may have been an amorphous substance which would not produce an x-ray diffraction pattern.

The capability of XRD was limited by the amount of material that could be lifted from the surface as a film. This limitation was most apparent for cathode WT-II, where analysis was not possible on the samples from the upstream end of the insert because a sufficient amount of material could not be obtained from the surface. Only in the region of the insert nearest the orifice was XRD able to reveal any information. The best correlation for the diffraction pattern was with the compounds molybdenum-rhenium or rhenium-tungsten. The similarity between the spectra for each compound made distinguishing between them difficult. Barium tungstate, $BaWO_4$, was also found on the surface; the compound probably came from the dark band of surface material that was observed during SEM examination (region 2, Fig. 18). The tungstate pattern was also found to be correlated with that of barium molybdate, $BaMO_4$, and, given the presence of the deposited molybdenum on

the insert surface, the formation of some amount of the molybdate may have occurred. The likelihood of molybdate formation was also applicable to the surface of the first wear-test cathode. Finally, a weak signal was found for the compound, Ba_2CaWO_6, which was an expected component of the chemistry of the 4:1:1 impregnate.

Material obtained from three different locations along the surface of cathode TL-I were analyzed. For region I (Fig. 19), the main compound found was the tungstate, $BaWO_4$, which may have been contained in the barium compound observed on the orifice plate. Tungsten metal was also detected. There were a few weak peaks which indicated that the tungsten oxide, WO_3, might be present. In the second region, $BaWO_4$ and tungsten were found. The tungstate must be part of the layer-like structures found on the insert surface. None of the tungsten oxides were detected in this region. The third region was found to contain only tungsten and possibly another tungsten oxide, WO_2. Some unidentifiable peaks were also found which may correlate layer formations that covered the surface in this area. Barium molybdate and molybdenum may have also been detected, but, due to difficulty in definitive pattern identification, it was uncertain.

The surface of the cathode TL-II insert was examined in a similar fashion (Fig. 20). However, the surface films from different locations were found to contain the same compounds. Peaks for tungsten were found, which was expected. In addition, barium tungstate was found over the entire surface of the insert; it may be part of the barium compound layer formations observed over much of the insert. Again, it was suspected that the molybdenum compounds might be present, since the molybdenum was found in several locations by EDS.

DISCUSSION OF RESULTS OF HOLLOW CATHODE EXAMINATION

The changes that the cathodes experienced during the extended tests included tungsten removal, deposition of tungsten or its oxide on the orifice channel, upstream orifice plate, and insert surfaces, formation of fiber-like crystal growth on the insert surface, formation of barium tungstate over regions of the insert surface, and formation of amorphous layers of barium compound over the upstream region of the insert surface. The potential of each of these phenomena to limit the long-life operation of the hollow cathodes will be addressed.

Tungsten removal: loss of material from the insert and the orifice plate could result in changing discharge characteristics by enlarging the orifice, with subsequent changes in cathode temperature and pressure, and in altering the emission characteristics of the insert by changing the surface work function. Orifice enlargement was not observed in any of the test cathodes, but material loss was found. The insert wall of cathode TL-I experienced the most severe material removal in the four cathodes examined. Thinning resulted in an approximately 11% increase in the insert inner diameter which decreased to a negligible diameter change at the upstream end. There was also an apparent increase in the surface porosity further upstream. This increase in porosity was observed in cathode TL-II at the downstream end, where the wall thickness was changed. Similarly, there was some material loss upstream of the large deposition in cathode WT-I. Cathode WT-II was the only cathode to have not experienced substantial tungsten removal from any surface. However, material loss was apparent in cathode WT-II in the removal of the initial surface layers of sintered tungsten, exposing the bulk tungsten and the pores between the grains which facilitated the transport of barium to the surface. Consequently, the tungsten removal cannot be seen as simply a destructive phenomenon.

However, deposition of tungsten, and possibly its oxide, are more likely to limit cathode operation, since deposition of the tungsten on internal surfaces could lead to changes in the discharge operation in two ways. First, significant deposition on the orifice resulting in a reduction in area would lead to a corresponding change in internal plasma conditions and emission characteristics. This change would result in higher cathode temperatures[15] which leads to reduced cathode lifetime. Secondly, deposition of material on the insert surface could plug the pores in the matrix and prevent barium from reaching the surface. This would result in an increased work function and therefore different operating characteristics in the affected

regions. Cathode WT-I was found to have experienced substantially more tungsten deposition at the orifice plate and insert surface than the second wear-test cathode (WT-II). While presently unproven, this change may be attributable to the improvement in the leakage rate of the propellant feed-system and to a different cathode activation procedure. The reduction in system leakage rate by 140% was not sufficient to eliminate tungsten deposition within the cathode completely, though the reduction in amount of deposited material was substantial and indicated that further improvements may prevent it from occurring. For cathode TL-I, tungsten was found deposited on the outer surface of the orifice plate, in the orifice chamfer and channel, and on the upstream side of the orifice plate. The deposition resulted in the effective elimination of the chamfer and extension of the orifice channel into the insert cavity. On the insert surface, there were multiple ridge-like structures of deposited material observed along the downstream region of the insert surface which were of substantial size. Cathode TL-II had similar ridge-like structures on the insert surface, though not as substantial as cathode TL-I. However, significantly more material was deposited into the orifice, onto the orifice plate, and into a plug which blocked the orifice. (It may be possible that the plug formation was a result of the keeper electrode destruction and high-voltage mode operation, as its presence would have made normal operation impossible if it restricted the propellant flow significantly.) In all, a substantial amount of tungsten was deposited on the internal surfaces of cathode TL-II, yet no source of this material was apparent. The large amount of material movement in the two thruster cathodes indicated that the cleanliness of their propellant feed-system, which was better than the first wear-test system, but worse than the second, was inadequate for extended discharge operation.

Finally, cathodes WT-I, TL-I, and TL-II all had fibrous tungsten growths both on large areas of the insert surface and in the gap between insert outer surface and cathode tube wall. The mechanism of formation of such deposition is not presently known. But, while the crystal growths observed between the insert outer surface and the cathode tube wall were very similar to the growths observed on the interior surface of the insert, their location outside and upstream of the insert surface would seem to preclude the same formation mechanism. Further data are required to make any assessment.

There were differences in the tungsten deposition in the wear-test cathodes and the life-test pair. First, cathodes WT-I and WT-II were both found to have tungsten deposited around the orifice in similar manners, though the degree of deposition was substantially different. However, neither of the cathodes TL-I or TL-II exhibited such a pattern of deposited tungsten. Material from the upstream sides of the orifice plates was removed instead. Secondly, the deposition found in the downstream end cathode WT-I was different than the deposition observed in either of the life-test cathodes in that the crystalline structure was not apparent. Again, no explanation for these differences is available.

A possible mechanism for the movement of tungsten within the cathode was tungsten oxide vapor transport. The formation of tungsten oxide, via reaction of the matrix tungsten with oxygen from contaminants and liberated oxygen from the cathode impregnate, was quite likely to occur on the insert surface. With surface temperatures in the range of 1000-1300 °C, the vaporization of the oxides will take place[16]. Using the methodology described by May[17] and data from Kohl[18] and Reick[19], vaporization rates for tungsten and tungsten oxides were determined. The tungsten vaporization rate was too low to account for the observable amount of material movement in the four cathodes at even the most extreme temperature conditions. However, the tungsten oxide vaporization rate was found to be at least 10^{15} times greater than the tungsten rate and would have resulted in more material movement than was observed. The limitation on the oxide vaporization may then be the amount of oxide available which was directly dependent on the level of feed-system contamination. Regardless, tungsten oxide vapor would be transported downstream in the propellant flow. Through some mechanism, the oxide was reduced and deposited. The crystalline formations observed in the cathodes may be indicative of the deposition of tungsten metal that had been reduced from the oxide state[20]. No explanation of the process of deposition, reduction of tungsten oxide to tungsten, and location of the deposited material sites can be offered at this time.

However, there are some factors which would be of importance. These include: gas/wall temperature, which may be linked to the reduction of tungsten oxide; localized pressure conditions, which may impact the vaporization and condensation rates of tungsten; and discharge activity, which would effect both temperature and pressure conditions. In addition, all of these factors would depend on the cathode geometry which seemed to change with time. Consequently, the listed factors would all be changing with time and discharge operation. Further data are needed to develop the explanations for the deposition phenomena.

Tungstate formation was an expected result of the reduction of the 4:1:1 impregnate through cathode operation-[7,21], though it is indicative of limited life. Cathode life limitation results from excessive tungstate formation. Since the reactions that take place are dependent on temperature, the localized formation of the tungstate in three of the cathodes indicated that these regions had the necessary conditions for formation. However, both thruster life-test cathodes were found to have tungstate over larger areas of the insert surface, particularly TL-II, which had tungstate present over the entire surface. Consequently, tungstate presence might be a result of movement of the material from formation sites to other locations on the insert surface. While tungstate formation was viewed as a limiting agent to cathode life and which should be eliminated, there was not enough evidence available which indicated that the emission processes were being affected in the cathodes or that tungstate formation was reduced on cathode WT-II as a result of operational upgrades.

The formation of amorphous barium compound layers on the insert was found to have occurred in all four cathodes, though it was more apparent on cathodes WT-I, TL-I, and TL-II. Given its composition being primarily tungsten and barium, with smaller amounts of calcium and aluminum, the material must result from the migrating of impregnate compounds to the surface where they reacted with the ambient environment to form into stable surface coatings. Since the cathode discharge was probably localized to the downstream end of the insert, no plasma activity took place in this region which might have led to further chemical reactivity and material removal. Also, temperatures in this region may have been lower than the emission area, which might affect the chemical processes. Regardless, the layers resulted from cathode operation and were probably still in place because the mechanisms for material removal that was evident in the downstream region of the insert surface were not active at the upstream end. Tungstate formation may have occurred in these layers, but, since the tungstate was not detected in all regions of the layer formation, the phenomena were probably not linked. In addition, exposure of the compound to atmospheric oxygen and moisture may have impacted its final composition. Until more evidence has been obtained, the mechanisms for formation of these layers and their significance will be open to speculation. These layers resembled in composition and appearance the material that was found in the insert-cathode gap in cathodes WT-I and TL-II. This material was believed to have affixed the inserts into the cathode body, and may have been formed by a similar process as the amorphous layers.

Molybdenum and rhenium were found in varying amounts over much of the insert surfaces in the cathodes TL-I and TL-II. The presence of these refractory materials was significant in two ways. First, the material has to have come from the cathode features upstream of the insert surface, indicating that removal of material from the cathode body tube, molybdenum insert collar, and electrical lead elements was occurring during discharge operation. Oxidation by propellant contaminants picked up in the feed-systems was a likely cause. This process was the probable source of the formation of the rhenium coating on the insert collar in the neutralizer cathode and which may also be linked to the differential deposition of molybdenum and rhenium on the upstream end of the insert. Secondly, these metals may have contributed to the cathode chemistry, particularly with the indicated presence of the barium molybdate, $BaMO_4$. One consequence of this refractory movement will be the reevaluation of the acceptability of the materials used for the cathode tube and insert support. However, more work is required in order to determine if these materials are having a significant impact on the insert condition.

CRITERIA DERIVED FROM RESULTS

The major life-limiting phenomenon observed in the four cathodes examined was the movement of tungsten on the insert and orifice plate surfaces which resulted in substantial changes in the cathodes's condition. The suspected cause of this movement was oxidation of the insert matrix tungsten by oxygen coming from contaminants in the propellant feed-system and being liberated from the insert impregnate. Feed-system contamination of the propellant was also the suspected source of oxidation of the other refractory metals within the cathode, molybdenum and rhenium, and their resulting movement into the insert region. Consequently, improving the system vacuum integrity should lead to a reduction in the tungsten removal and deposition.

Barium tungstate and molybdate formations were found in all of the cathodes. However, sufficient quantitative data do not exist to indicate definitively that excessive tungstate formation had occurred. Therefore, the importance of the formation of the tungstates and other barium alloys as limiters in cathode longevity cannot be judged at this time.

In spite of the lack of a complete understanding of the cathode chemistry, the data obtained from the four hollow cathodes suggested some criteria for the systems used to operate these devices. Several improvements were observed in the cathode condition, both in terms of operational characteristics of the discharge and in the final condition of the cathode and its insert, after the second wear-test. In addition, the starting characteristics of the discharge were found to have been improved substantially. Ignition of the discharge no longer required the use of increased propellant flow or high voltages for electrical breakdown. These improvements are believed to have resulted from two changes. First, upgrading the propellant feed-system in order to improve its vacuum integrity, resulting in a decrease in oxygen-bearing contaminants that might reach the cathode. While the contributors to propellant contamination need to be quantified, the destructive effects observed might be a leakage issue alone, which would be resolved by system changes. Secondly, the use of an activation procedure based on the procedure used in the SEPS program to ensure proper activation/reactivation of the insert surface. Therefore, given the observed changes in cathode operation and condition, the suggested criteria for extended cathode operation are:

- Reduce overall length of the feed-lines which results in a reduction in area for potential outgassing and lowered fitting count.

- Avoid the use of flexible feed-lines made of elastomer materials, in order to minimize outgassing and ensure vacuum-quality seals.

- Use vacuum fittings and components wherever possible to improve the propellant feed-system vacuum integrity.

- Use larger diameter feed-lines. While the surface area increases with diameter, the evacuation rate of the system increases as the cube of the radius, resulting in more effective removal of outgassing products.

- Reduce impact of outgassing by using a technique to clean the internal feed-system surfaces, such a heating or reactive gas cleaning.

- Use materials for cathode fabrication which will not impact upon cathode operation.

- Use the SEPS-based procedure for cathode activation and reactivation after exposure to atmosphere. As the process is quite lengthy, it is possible that a more compact procedure can be defined through further effort.

CONCLUSION

The work reported in this paper consisted of the analysis and examination of four hollow cathodes using microanalysis techniques in order to characterize the life-limiting phenomena that resulted from their extended operation. The first pair of cathode examined were operated for approximately 500 hours in an ion thruster simulator at a 5.0 kW-equivalent power level using different cathode activation and propellant

feed-system procedures. The changes in cathode operating characteristics and feed-system integrity were documented. The second pair of cathodes were the main discharge cathode and neutralizer cathode from an ion thruster which had completed an 890-hour life-test at a 5.5 kW power level. The observed changes to the cathode and insert surfaces resulting from extended operation have been documented.

Several common phenomena were observed among the four cathodes. The greatest change to the cathode condition was found to be removal of refractory metals, primarily tungsten, and their subsequent deposition on other cathode surfaces. This material removal and deposition was substantial on the orifice and insert surfaces of the first wear-test and both thruster life-test cathode, but was reduced in the second wear-test cathode. Barium tungstate and possibly barium molybdate were also found in all four cathodes. Correlation of feed-system condition with the resulting changes to the cathodes led to criteria for the improvement of vacuum integrity. In addition, the use of a SEPS-derived cathode activation procedure has resulted in improvements in cathode discharge ignition. These criteria for improved cathode longevity and discharge operation are proposed for use in hollow cathode and full thruster testing facilities.

Acknowledgements: The efforts of John E. Eckert, John R. Miller, Gerald F. Schneider, and Clifford H. Schroeder for technical support of SBJ1 testing and Ruth E. Cipcic for performance of x-ray diffraction analysis are gratefully acknowledged.

REFERENCES

1. Kaufman, H.R., "Technology of Electron-Bombardment Thrusters" in *Advances in Electronics and Electron Physics*, *36*, L. Marton, ed. New York: Academic, 1974, pp. 265-373.

2. ___, "30-cm Ion Thrust Subsystem Design Manual," NASA TM-79191, 1979.

3. Mirtich, M.J., and Kerslake, W.R., "Long Lifetime Hollow Cathodes for 30-cm Mercury Ion Thrusters," AIAA paper 76-985, Nov. 1976.

4. Mantenieks, M.A., "Hg Ion Thruster Component Testing," AIAA paper 79-2116, Oct. 1979.

5. Collett, C., "Thruster Endurance Test," Hughes Research Labs., NASA CR-135011, May 1976.

6. Kohl, W.H., *Handbook of Materials and Techniques for Vacuum Devices*, New York: Reinhold, 1967, pp. 494.

7. Lipelas, R.A., and Kan, H.K.A., "Chemical Stability of Barium Calcium Aluminate Dispenser Cathode Impregnants," Applications of Surface Science, **16**, 1983, pp.189.

8. Siegfried, D.E., "A Phenomenological Model for Orificed Hollow Cathodes," NASA CR-168026, Dec. 1982.

9. Brophy, J.R., and Garner, C.E., "Tests of High Current Hollow Cathodes for ion engines," AIAA paper 88-2913, July 1988.

10. Rawlin, V.K., "Internal Erosion Rates of a 10 kW Xenon Ion Thruster," AIAA paper 88-2912, July, 1988.

11. Verhey, T.R., and MacRae, G.S., "Requirements for Long-Life Operation of Inert Gas Hollow Cathodes-Preliminary Report," AIAA Paper 90-2586, July, 1990.

12. Patterson, M.J., and Verhey, T.R. "5 kW Xenon Ion Thruster Life-test," AIAA Paper 90-2543, July, 1990.

13. DePauw, J.F., "30cm Thruster Cathode Activation," NASA TRIM No. 13, Dec. 1977.

14. O'Hanlon, J.F., *A User's Guide to Vacuum Technology*, New York: John Wiley & Sons, 1989, pp. 97.

15. Rawlin, V.R., Patterson, M.J., Chopra, A., and Martin, S.M., "High Current Hollow Cathodes for Ion Thrusters," AIAA Paper 87-1072, May, 1987.

16. Reick, G.D., *Tungsten and its compounds*, Oxford: Pergamon Press, 1967, pp. 96.

17. May, C.E., "Calculation of Vaporization Rates Assuming Various Rate Determining Steps: Application to the Resistojet," NASA TM-83757, Aug. 1984.

18. Kohl, op.cit., pp. 260.

19. Reick, op.cit., pp. 20.

20. Ohlinger, W., Personal communication, May, 1991.

21. Ohlinger, W., Personal communication, March, 1991.

Table I. Summary of hollow cathode design specifications

Cathodes	Test Configurations	Dimensions
WT-I WT-II TL-I	SBJ1 thruster simulator; 504 hr. wear-test SBJ1 thruster simulator; 478 hr. wear-test Ion thruster; 890 hr. life-test	Body Tube: Material: Mo-41-Re tubing Diameter: 0.64 cm Length: 10.2 cm Wall Thickness: 0.046 cm Orifice Plate: Material: W/2%Th Thickness: 0.13 cm Orifice Size: 0.15 cm Chamfer: 45° Electron-beam welded to body tube.
TL-II	Ion thruster; 890 hr. life-test	Body Tube: Material: Mo-41-Re tubing Diameter: 0.64 cm Length: 6.4 cm Wall Thickness: 0.046 cm Orifice Plate: Material: W/2%Th Thickness: 0.13 cm Orifice Size: 0.05 cm Chamfer: 45° Electron-beam welded to body tube.
Insert	All tests	Insert body: Material: Sintered W; 80% porosity Outer diameter: 0.53 cm Inner diameter: 0.38 cm Length: 2.54 cm Impregnate: 4:1:1 mixture of $BaO \cdot CaO \cdot Al_2O_3$ Mo Collar: Outer diameter: 0.53 cm Inner diameter: 0.36 cm Length: ~0.2 cm Brazing material: Mo-Ru

Table II. Summary of hollow cathode operational parameters.

	Operating Parameters			
Test Cathodes	Emission Current (A)	Discharge Voltage (V)	Propellant Flowrate (sccm)	Tube Temperature (°C)
WT-I				
bot:	--	14.9	--	1160
eot:	--	19.4	--	1214
mean:	23.0	17.9	6.1	1162
WT-II				
bot:	--	22.6	--	1143
eot:	--	18.0	--	1084
mean:	23.0	19.7	6.1	1098
TL-I				
bot:	--	27.3	4.0	--
eot:	--	27.0	4.6	--
mean:	18.8	26.9	4.3	--
TL-II				
bot:	5.8	13.5	3.3	--
eot:	6.15	17.0	5.2	--
mean:	5.9	15.4	4.7	--

bot - beginning of test value
eot - end of test value
mean - average value during test

Table III. Summary of ion thruster life-test shut-down history.

Event	Time(hrs.)	Shut-down Conditions	Re-ignition Procedure
1	184.5	High-voltage recycle	None Required
2	291.5	Main and neutralizer discharges shut off intentionally.	Reactivated Cathode: - 10 sccm xenon purge - heater turned on and current raised in to 2.0 A increments over an hour to 9.0 A max.
			Ignition: - raised neutralizer cathode flow to 130 sccm. - raised main cathode flow to 33 sccm. - pulsed main cathode igniter. - lit both cathodes.
3	317.7	Only neutralizer discharge was extinguished.	Reactivated by standard procedure. - ignited with 380 V applied to keeper.
4	441.4	Main and neutralizer discharges lost.	Reactivated and ignited same as event #2, except neutralizer cathode flow was not raised as high.
5	572.4	Main cathode discharge lost.	Re-ignited with 3.0 kW pulse. - no activation required
6	576.6	Main cathode discharge lost.	Same as event #5.
7	625.0	Main cathode discharge lost.	Same as event #5.

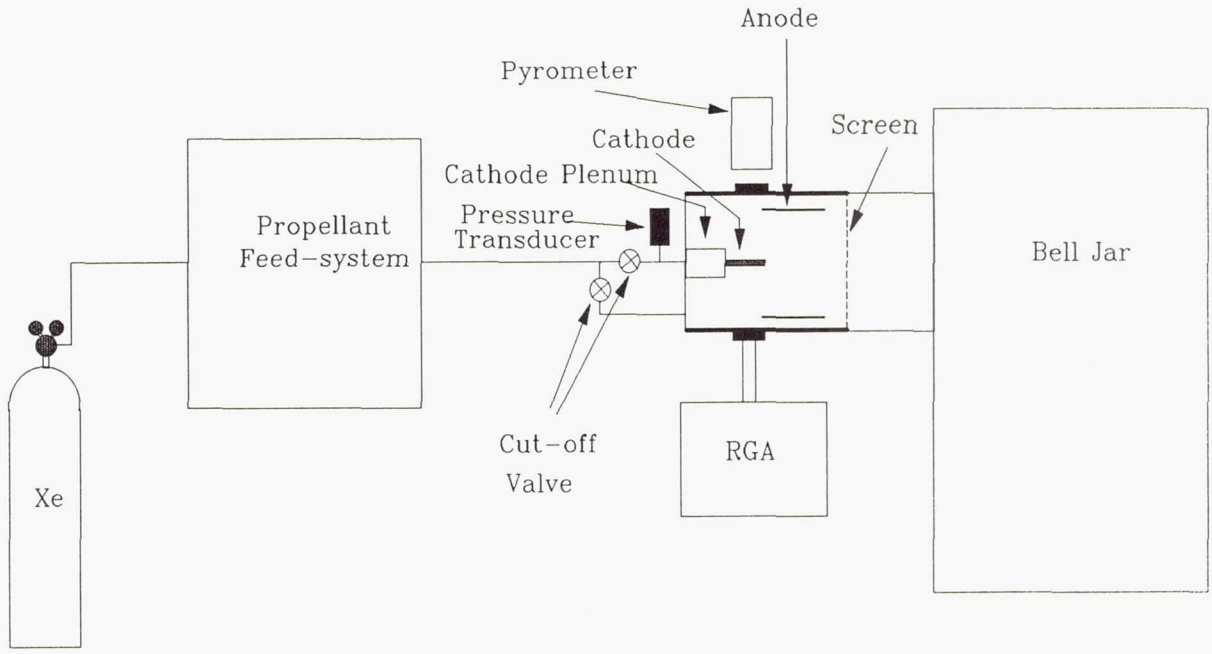

Figure 1. Schematic of SBJ1 Test facility.

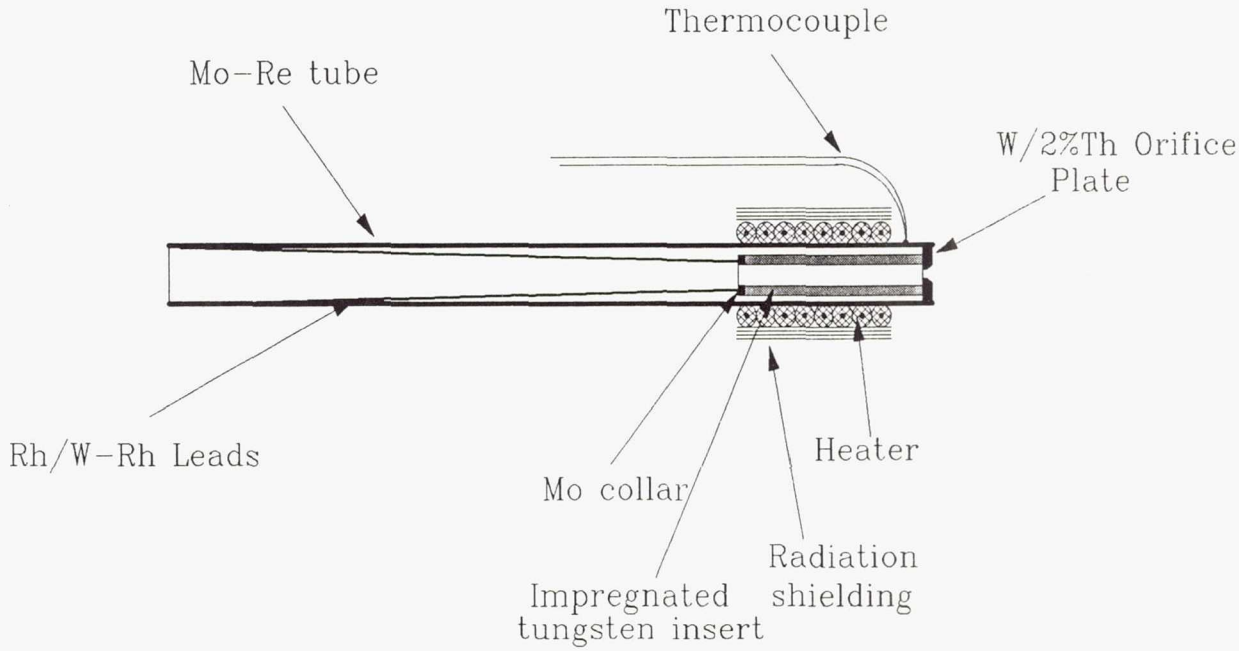

Figure 2. Cross-section of hollow cathode.

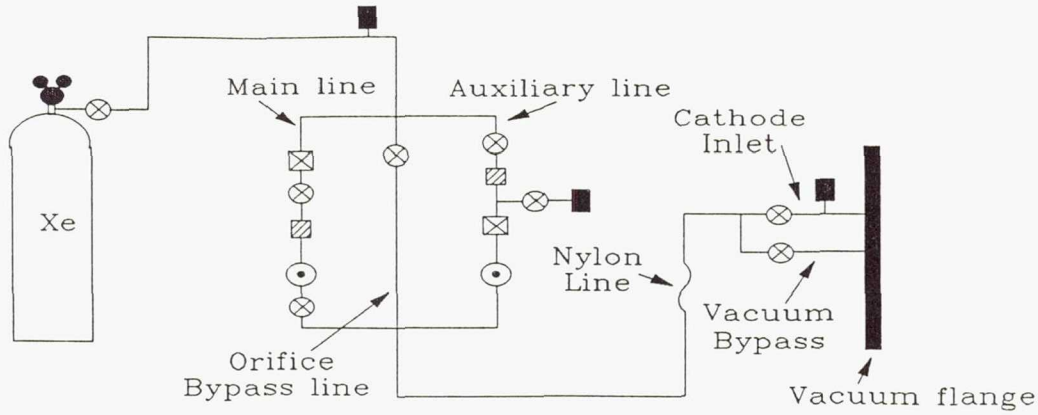

Legend:

⊗ – Cut–off valve
⊙ – Metering Valve
▨ – Flowmeter
■ – Pressure Tansducer
⊠ – Solenoid Valve
– Pressure Regulator

Figure 3. Schematic of SBJ1 propellant feed-system.

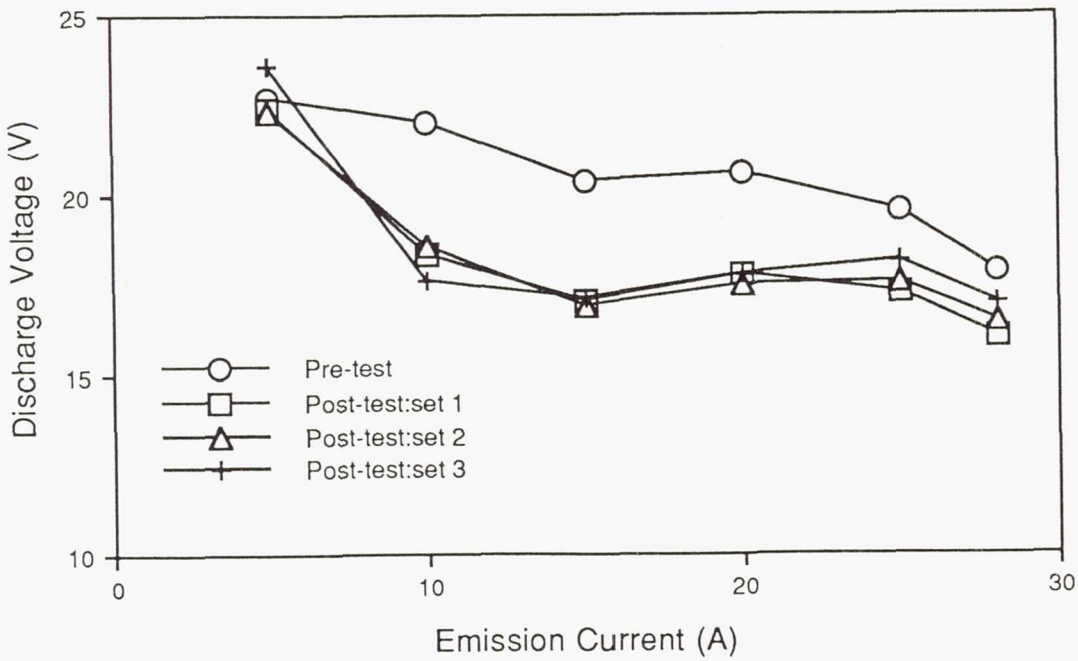

Figure 4. Discharge voltage vs. emission current for cathode WT-II. All data was taken at a xenon flow rate of 6.1 sccm. Post-test data was taken at ends of wear-test segments (set 1 & 2) and after extended exposure to atmosphere and reactivation (set 3).

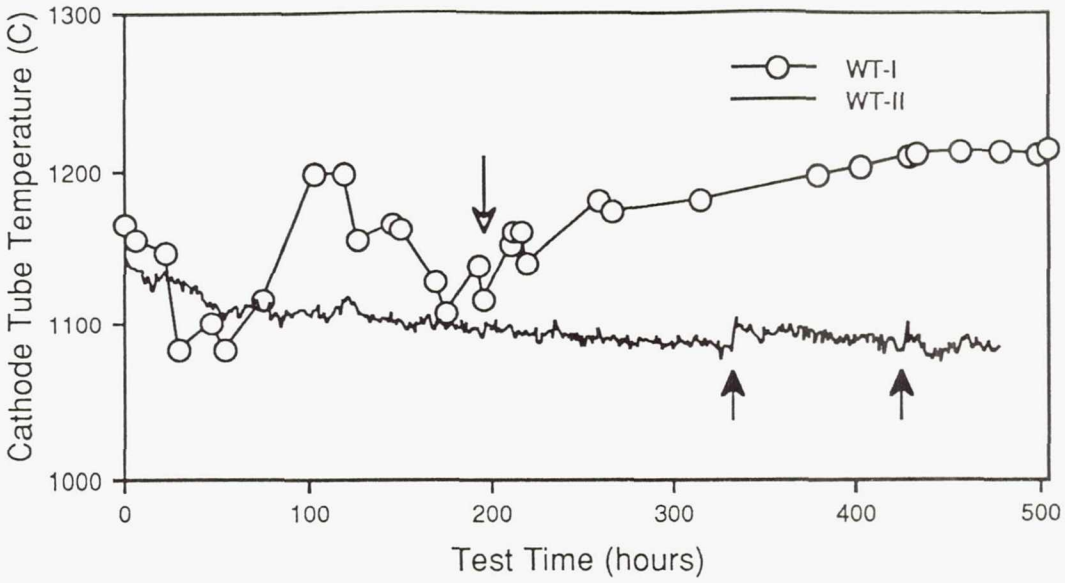

Figure 5. Cathode tube temperatures over course of two SBJ1 wear-tests. The emission currents were 23.0 A and xenon flow rates were 6.1 sccm. Test shut-downs for cathodes WT-I and WT-II are indicated by the open and solid arrows, respectively.

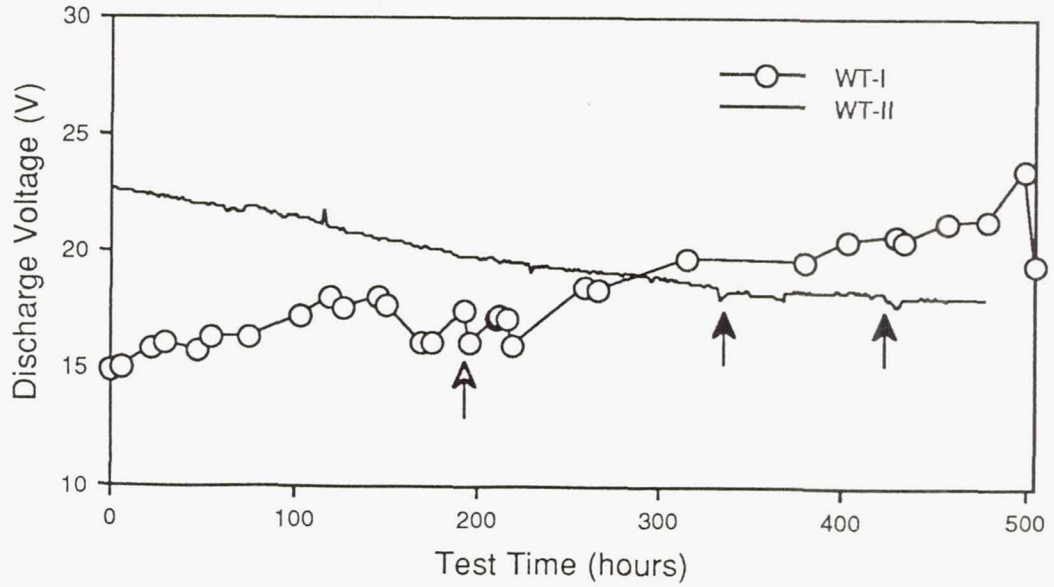

Figure 6. Discharge voltage over the course of two SBJ1 wear-tests. The emission currents were 23.0 A and xenon flow rates were 6.1 sccm. Test shut-downs for cathodes WT-I and WT-II are indicated by the open and solid arrows, respectively.

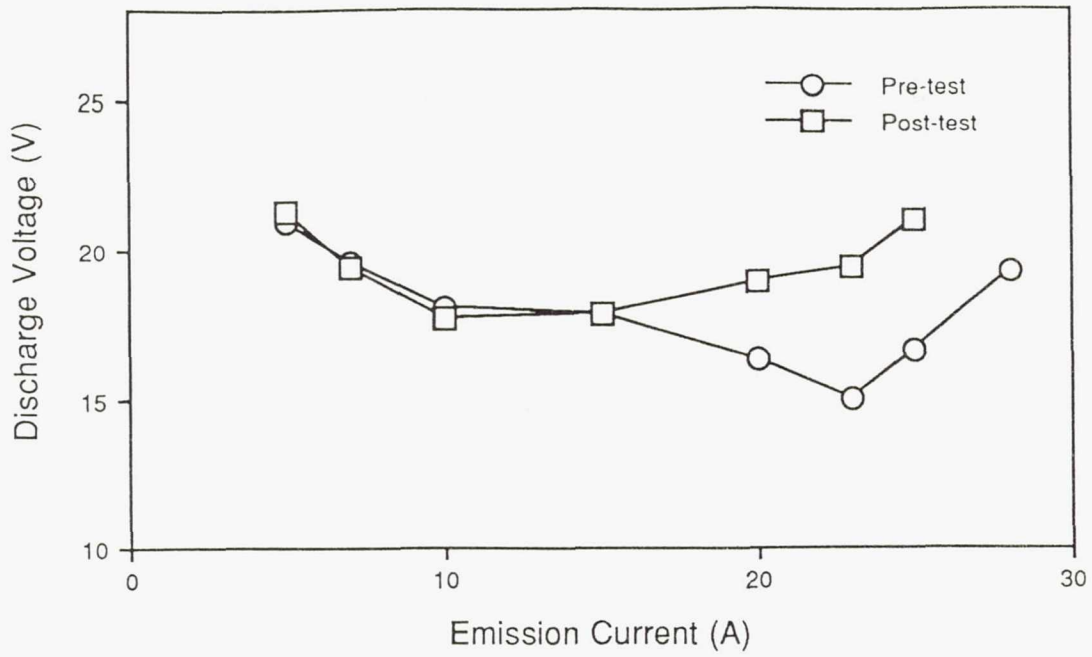

Figure 7. Discharge voltage vs. emission current for cathode WT-I. All data was taken at a xenon flow rate of 6.1 sccm.

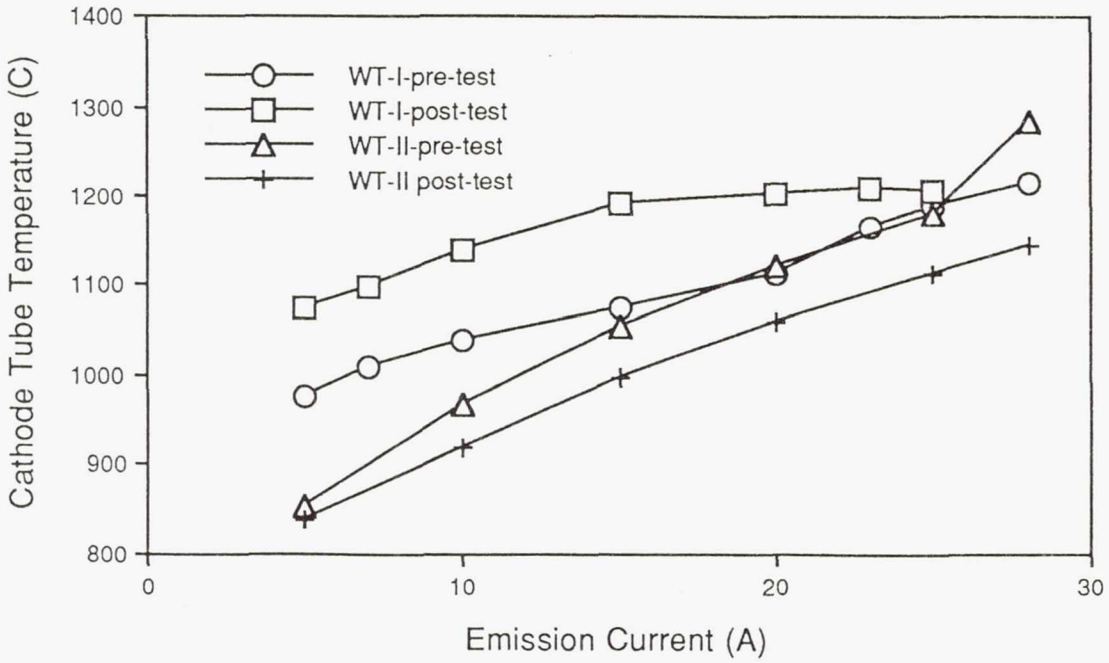

Figure 8. Cathode tube temperatures vs. emission current for cathodes WT-I and WT-II. All data taken at a xenon flow rate of 6.1 sccm.

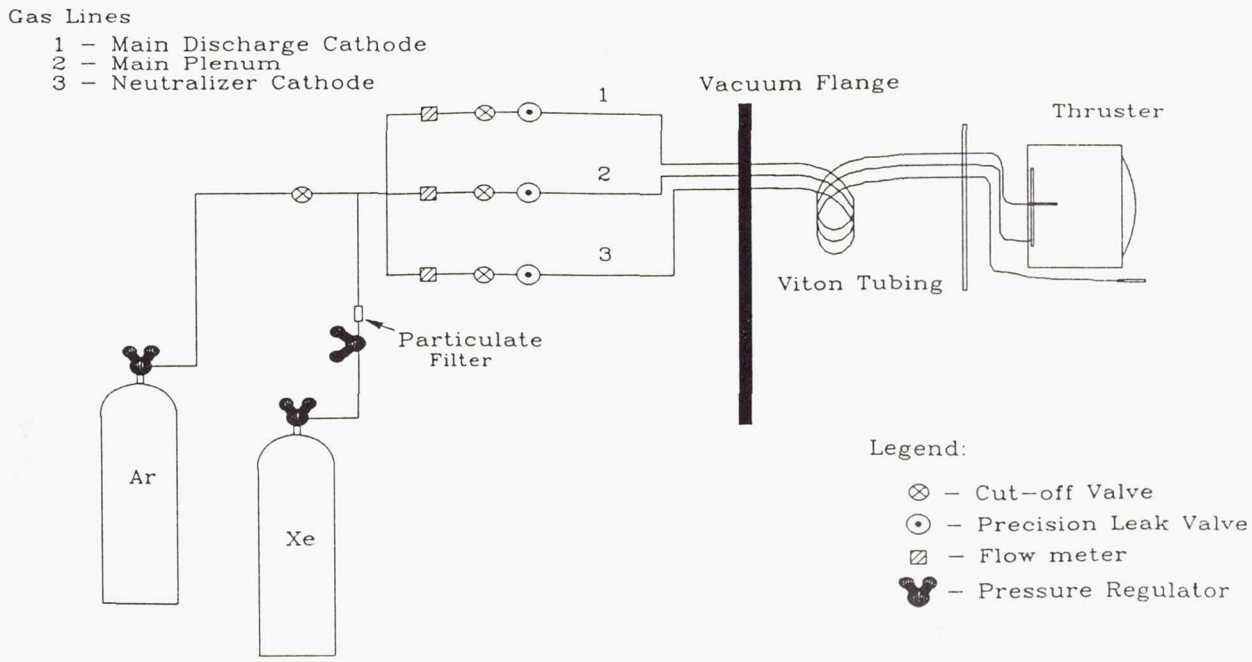

Figure 9. Schematic of Ion Thruster Life-test Propellant Feed-system.

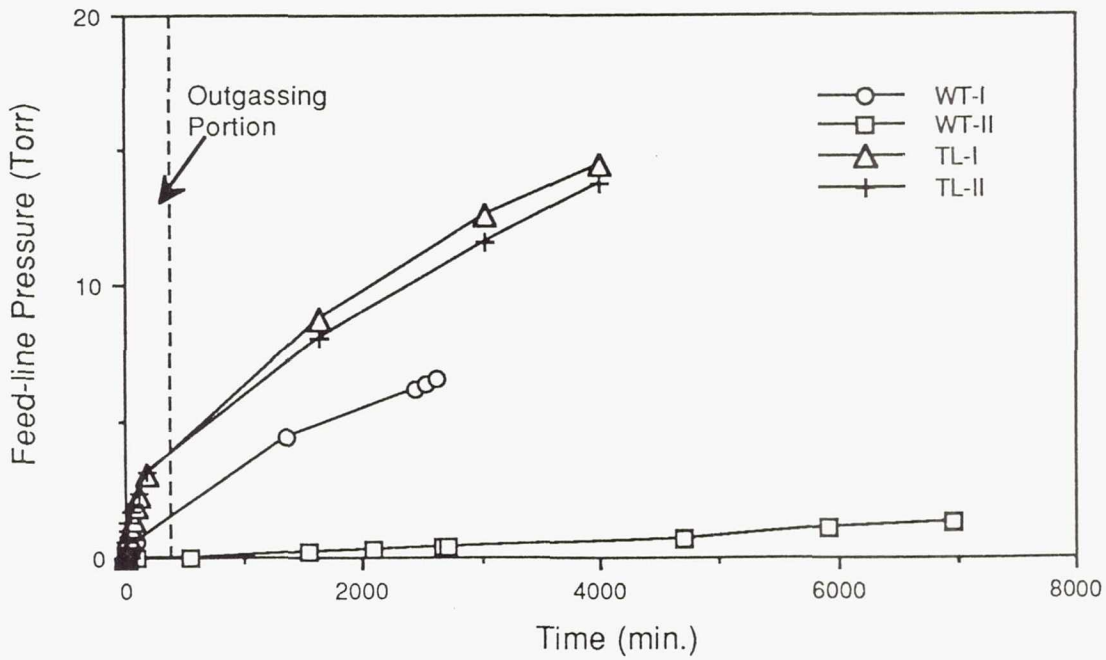

Figure 10. Feed-line pressure vs. time for leakage rate determination for the propellant feed-systems for both SBJ1 wear-tests and the thruster life-test cathode feed-lines.

(a) Prior to Testing

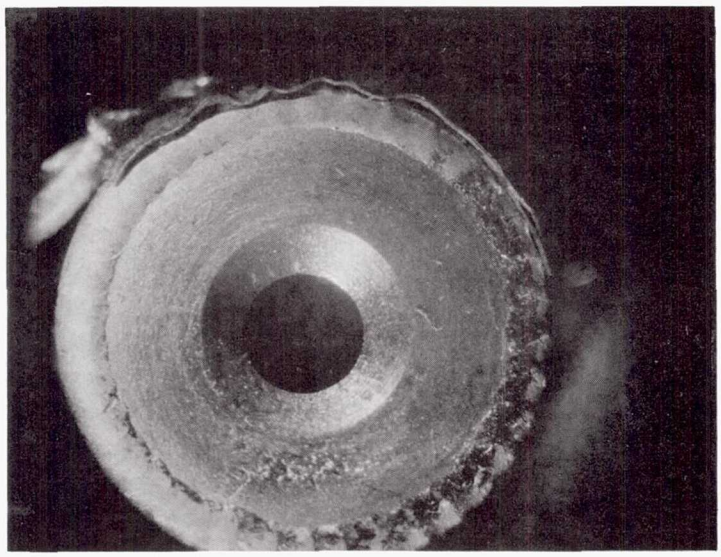

(b) After Testing

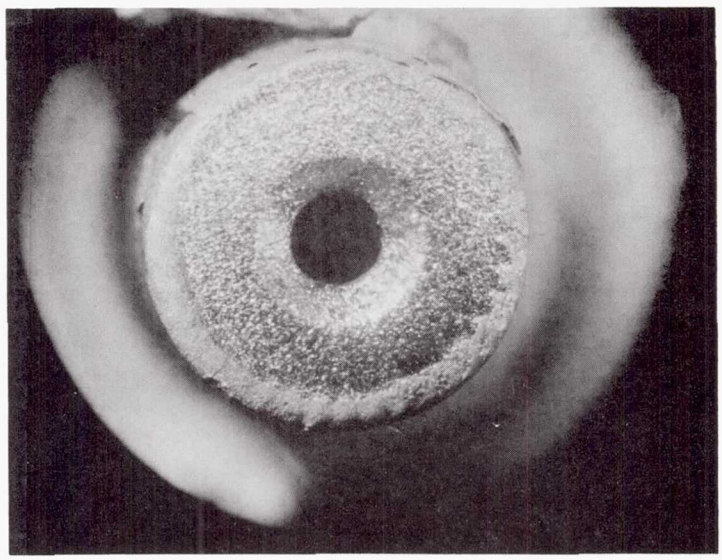

Figure 11. External surface of cathode WT-I orifice plate.

(a) Prior to Testing

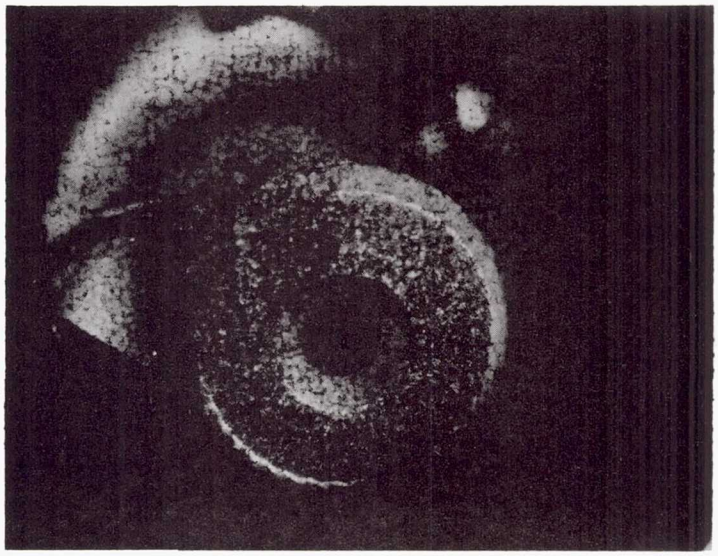

(b) After Testing

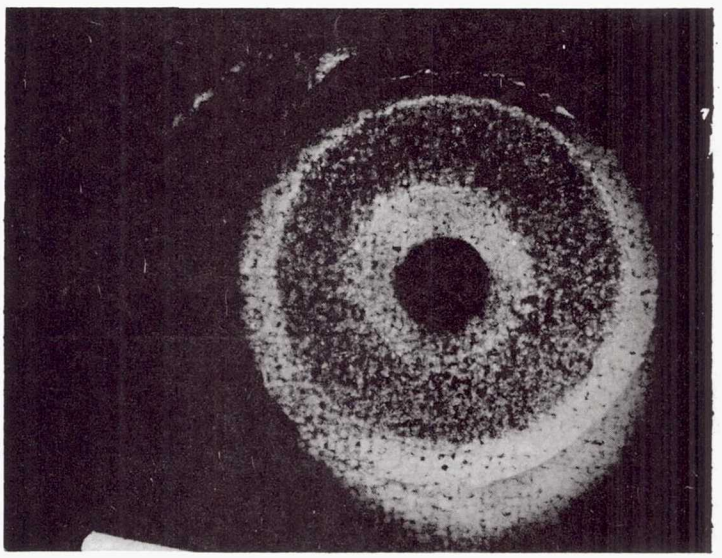

Figure 12. External surface of cathode WT-II orifice plate.

(a) Prior to Testing

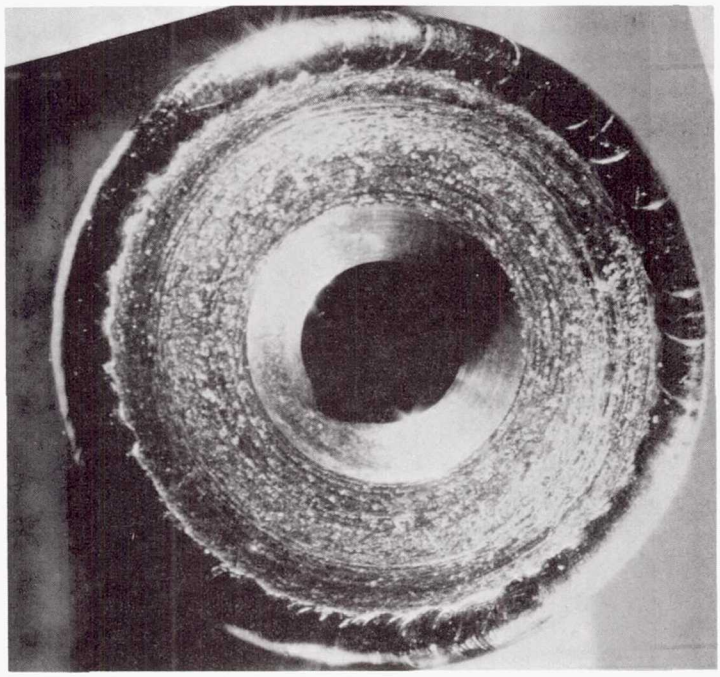

(b) After Testing

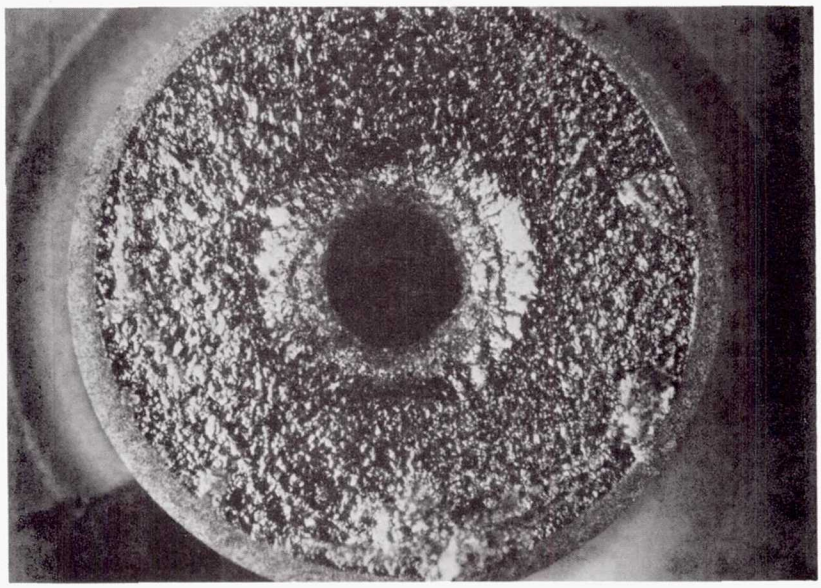

Figure 13. External surface of cathode TL-I orifice plate.

(a) Prior to Testing

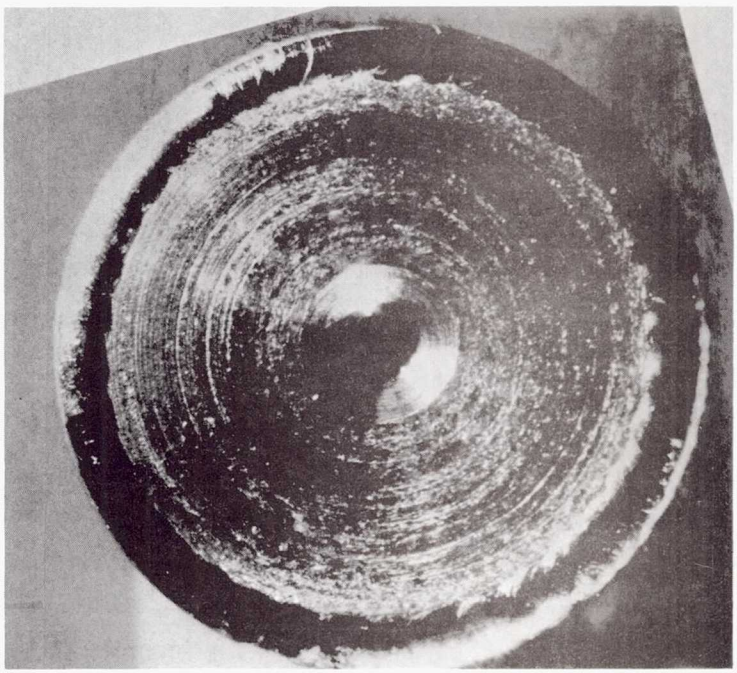

(b) After Testing

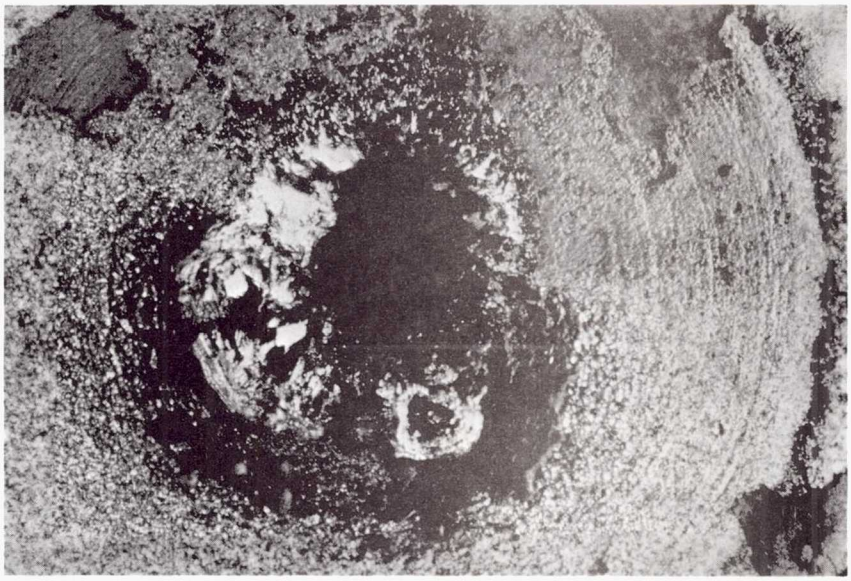

Figure 14. External surface of cathode TL-II orifice plate.

(a) WT-I Cathode

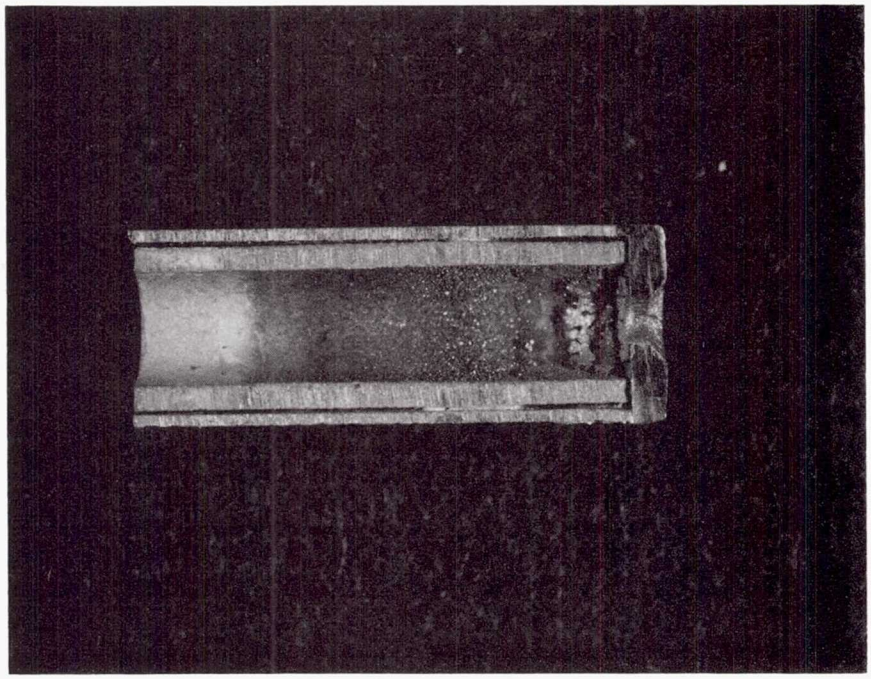

(b) WT-II Cathode

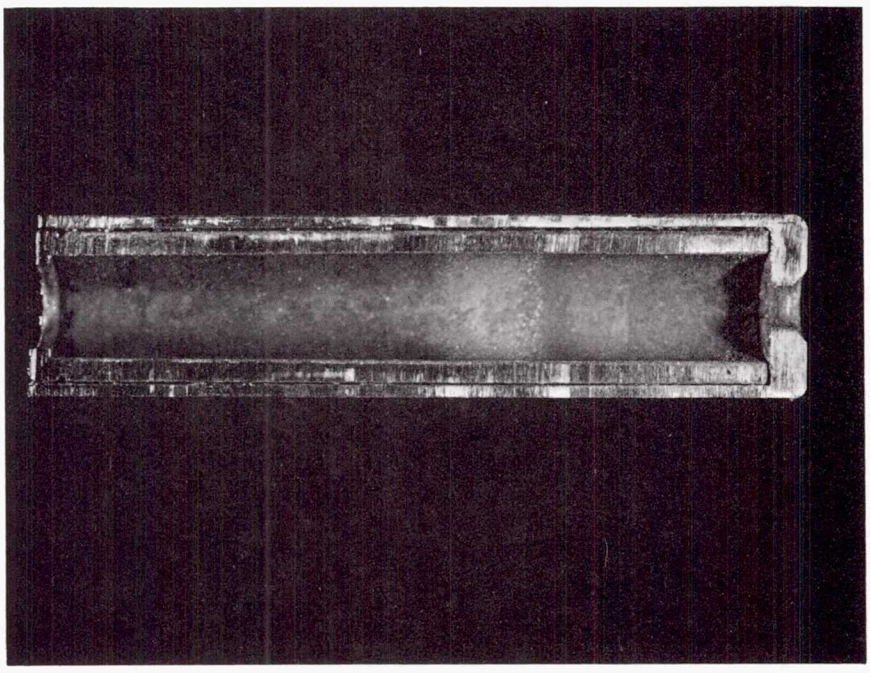

Figure 15. Sliced SBJ1 wear-test cathodes. Gas flowed from left to right.

(a) TL-I Cathode

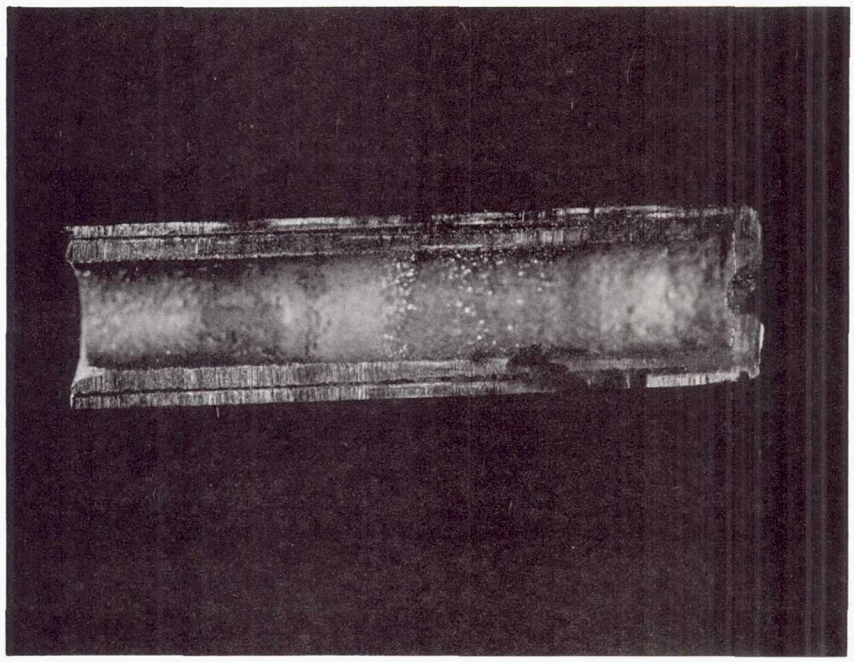

(b) TL-II Cathode

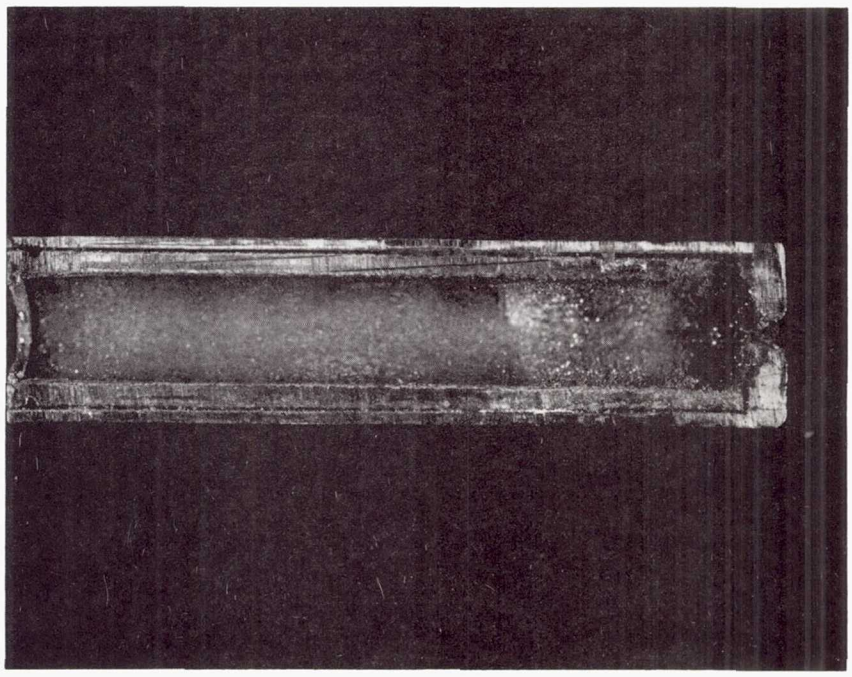

Figure 16. Sliced thruster life-test cathodes. Gas flowed from left to right.

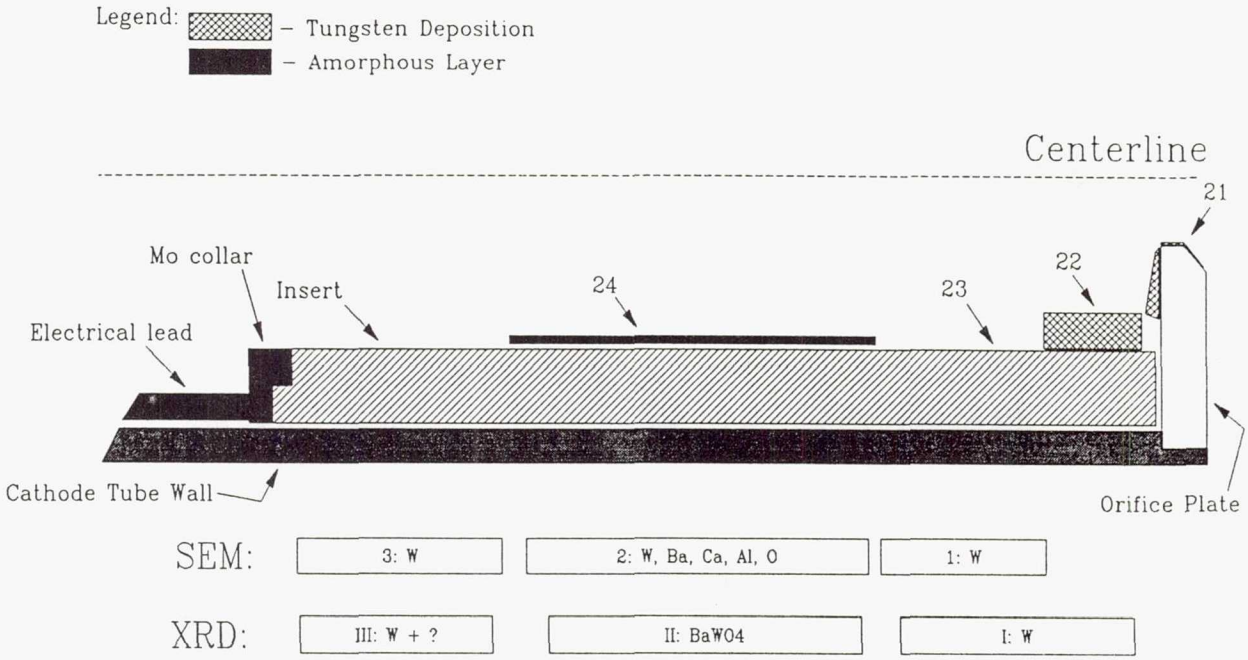

Figure 17. Schematic of cathode WT-I cross-section with the observed phenomena summarized. Numbers locate the SEM photographs by figure number and the SEM and XRD bars list the elemental and molecular composition in respective regions.

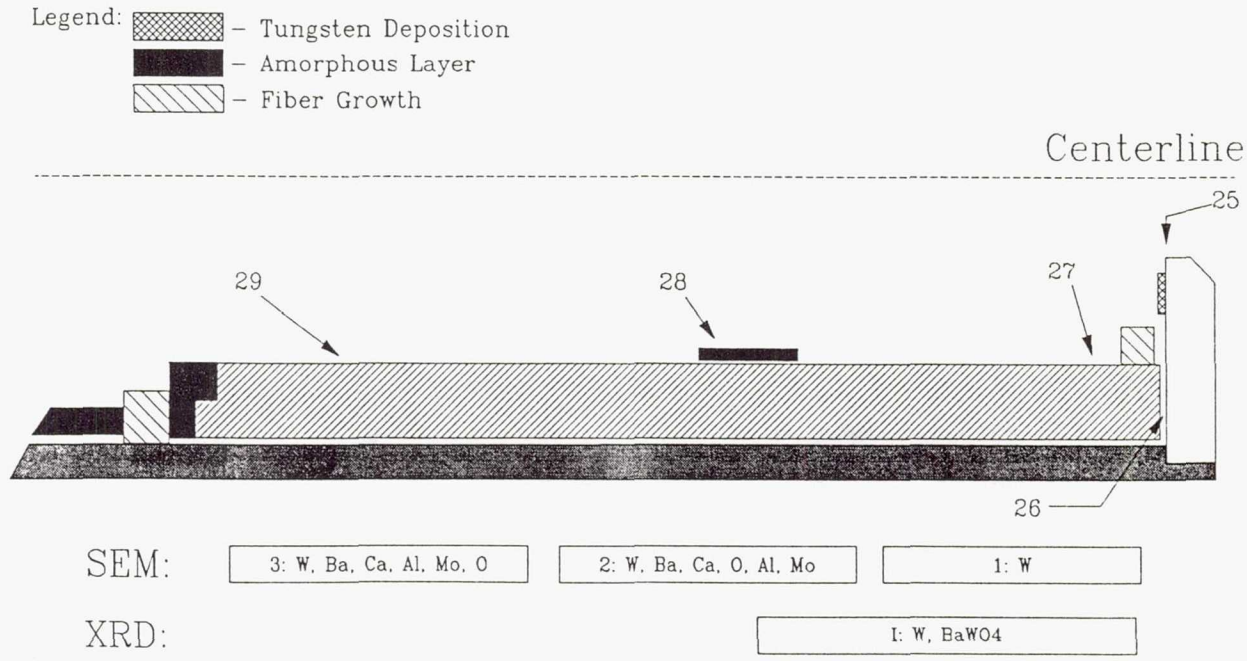

Figure 18. Schematic of cathode WT-II cross-section with the observed phenomena summarized.

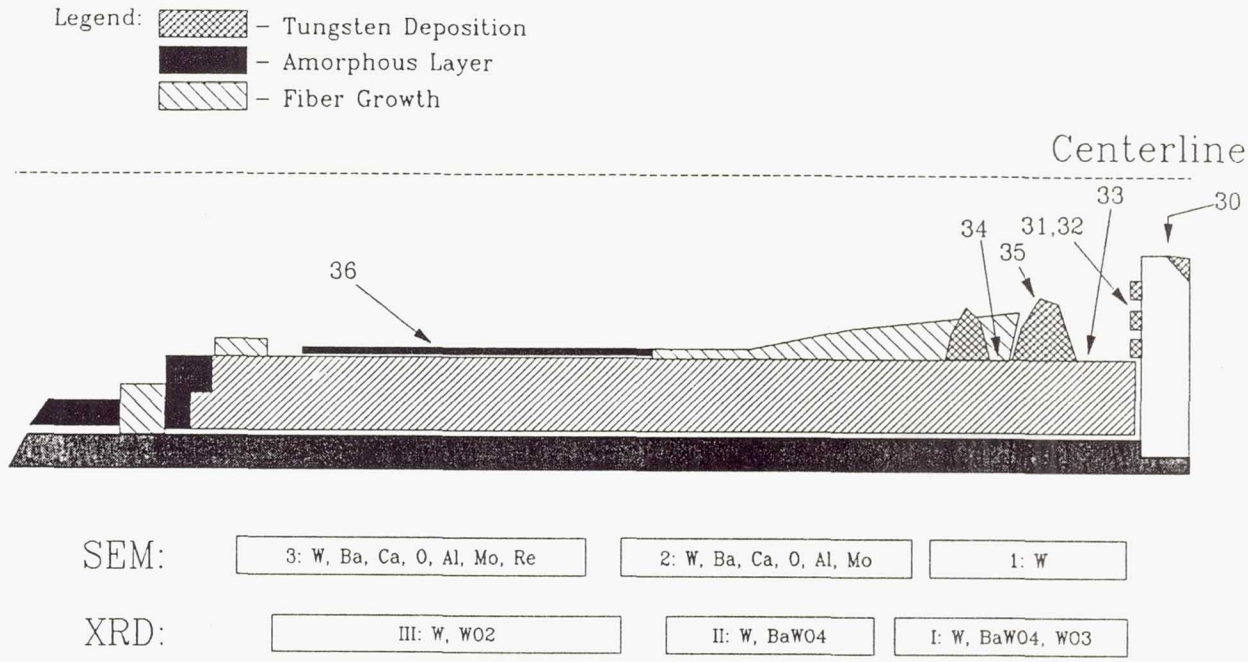

Figure 19. Schematic of cathode TL-I cross-section with the observed phenomena summarized.

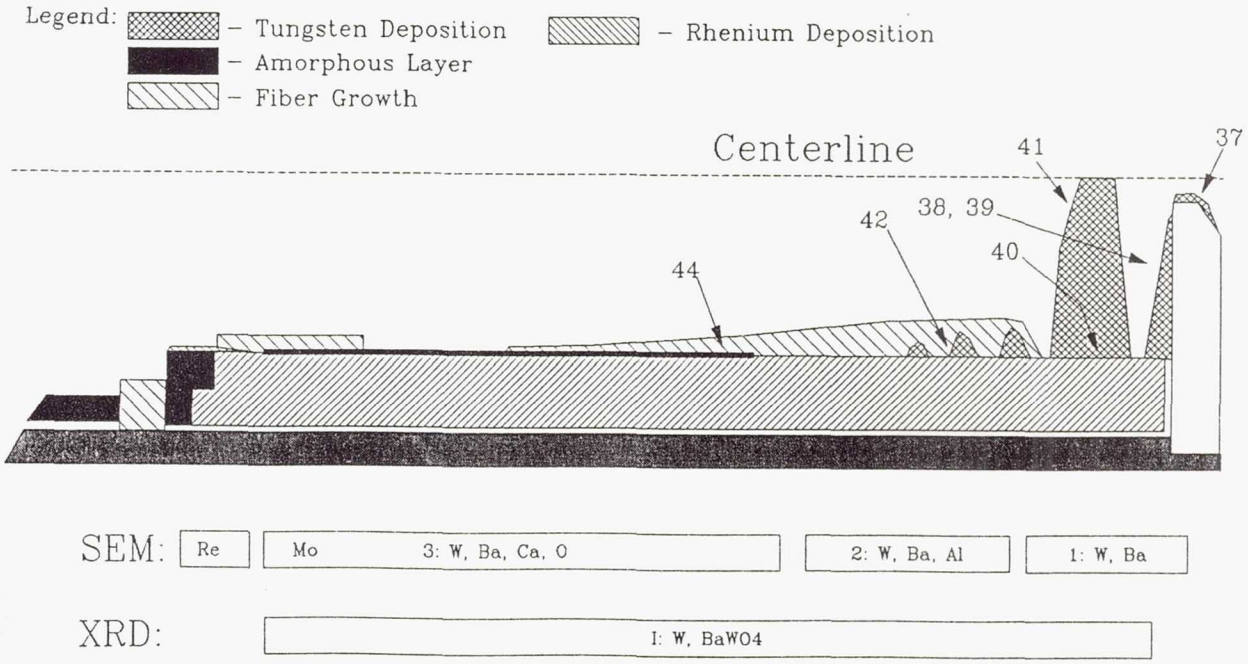

Figure 20. Schematic of cathode TL-II cross-section with the observed phenomena summarized.

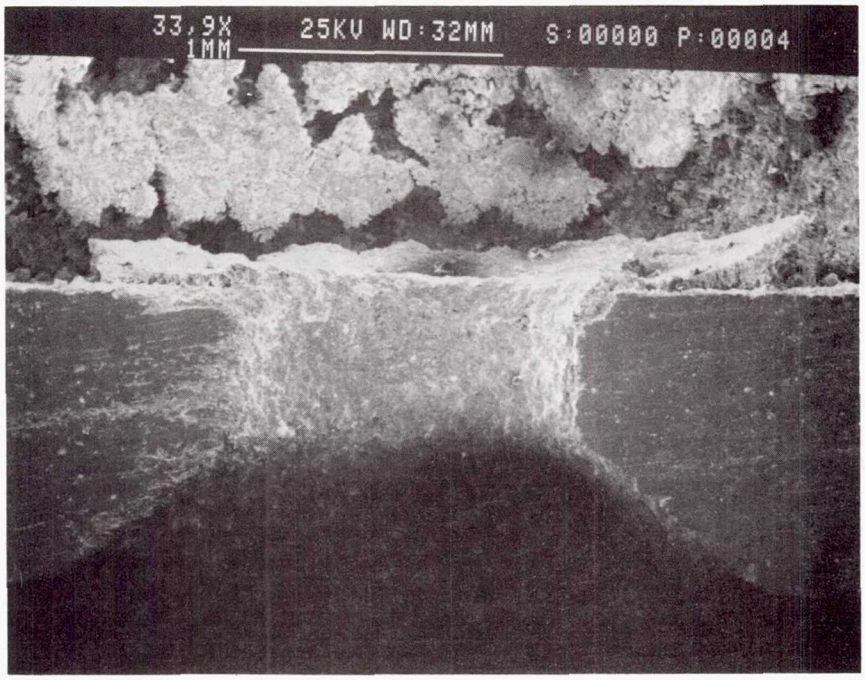

Figure 21. SE image of the orifice channel of cathode WT-I. Propellant flowed from top to bottom.

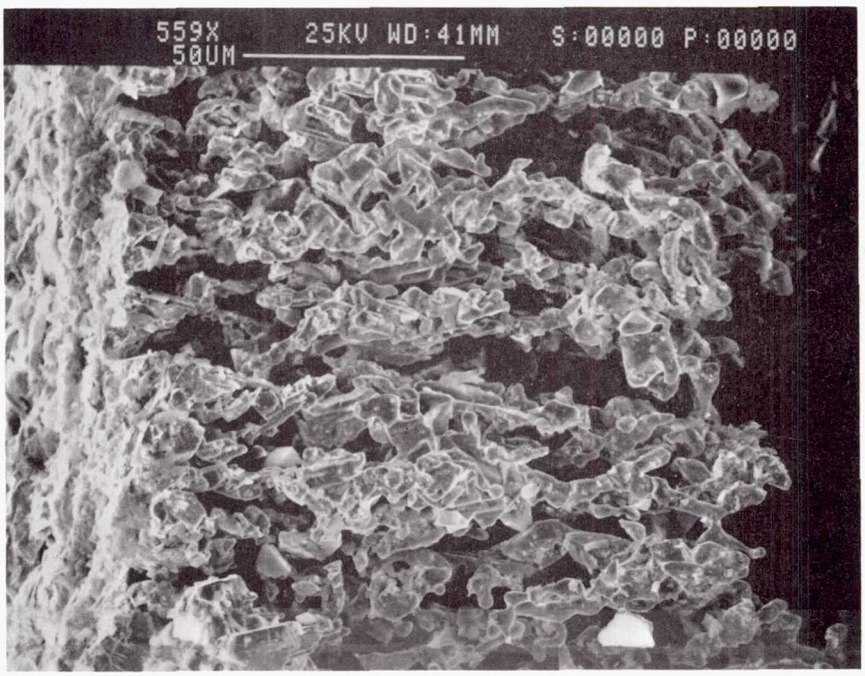

Figure 22. SE image of the tungsten deposition on the downstream end of cathode WT-I. The top of the deposition surface is at the left of the photograph.

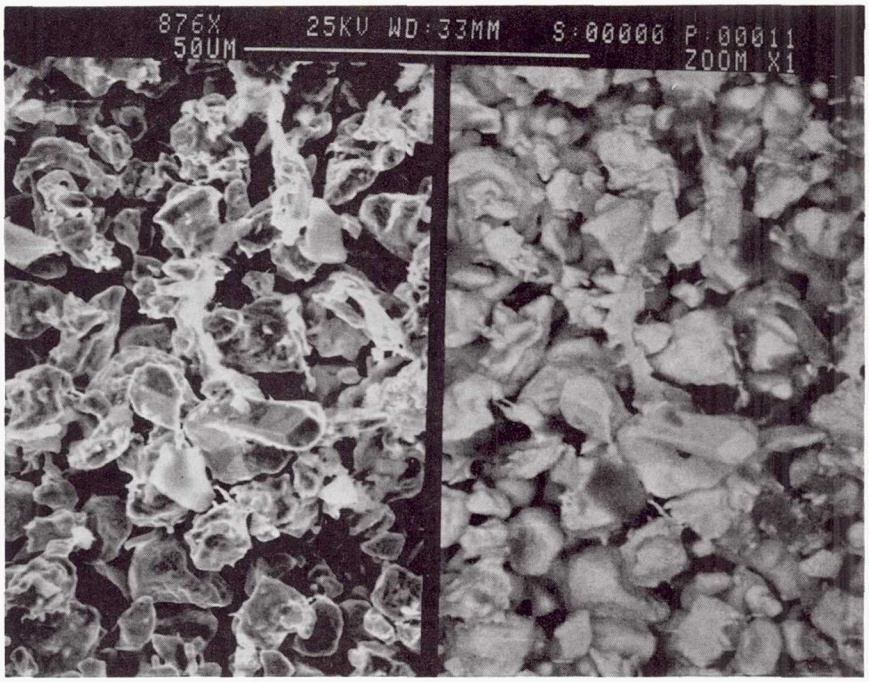

Figure 23. Surface of the second region of cathode WT-I insert, showing grain structures, SE image on the left and BSE image on the right.

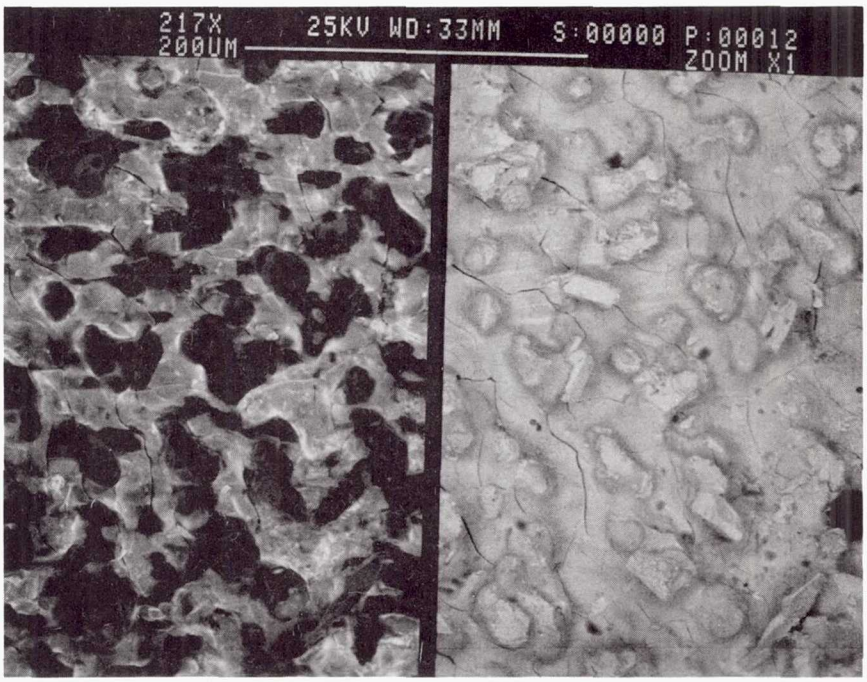

Figure 24. Nonconductive material on the surface of the third section of cathode WT-I insert, SE image on the left and BSE image on the right.

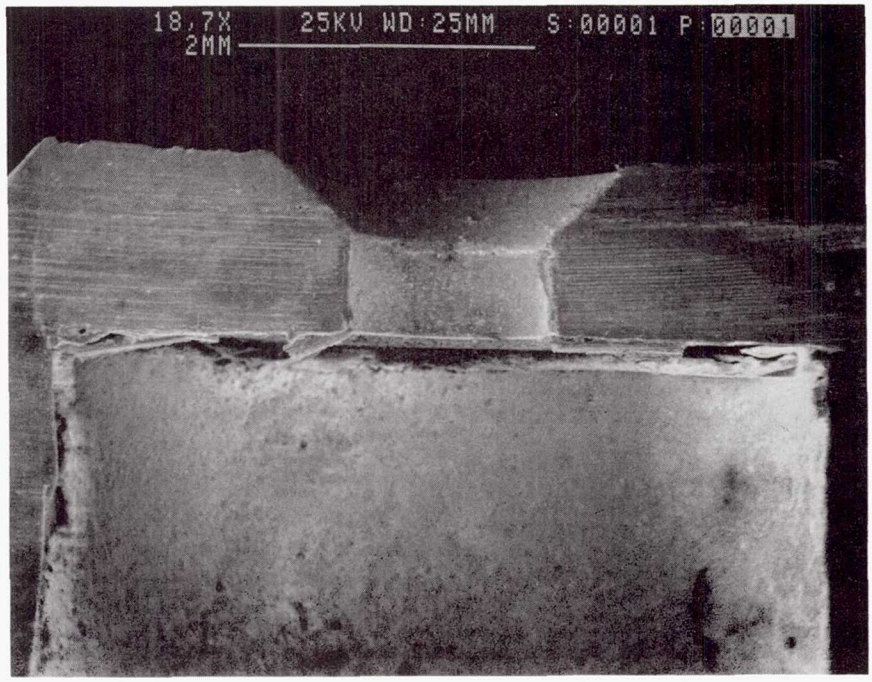

Figure 25. SE image of orifice of cathode WT-II. Propellant flowed from bottom to top.

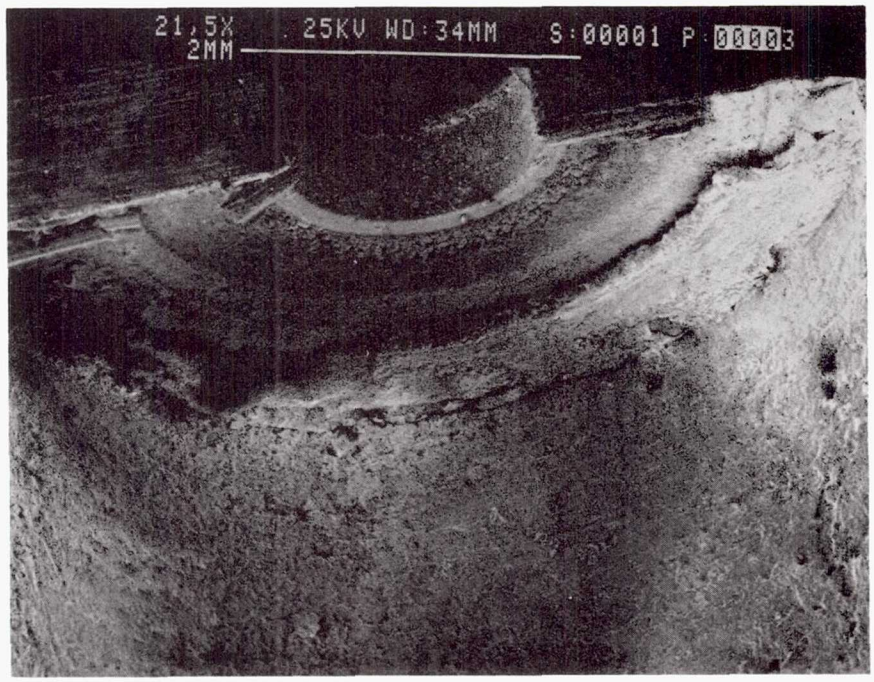

Figure 26. SE image of the inside of cathode WT-II tube without the insert. Propellant flowed from bottom to top.

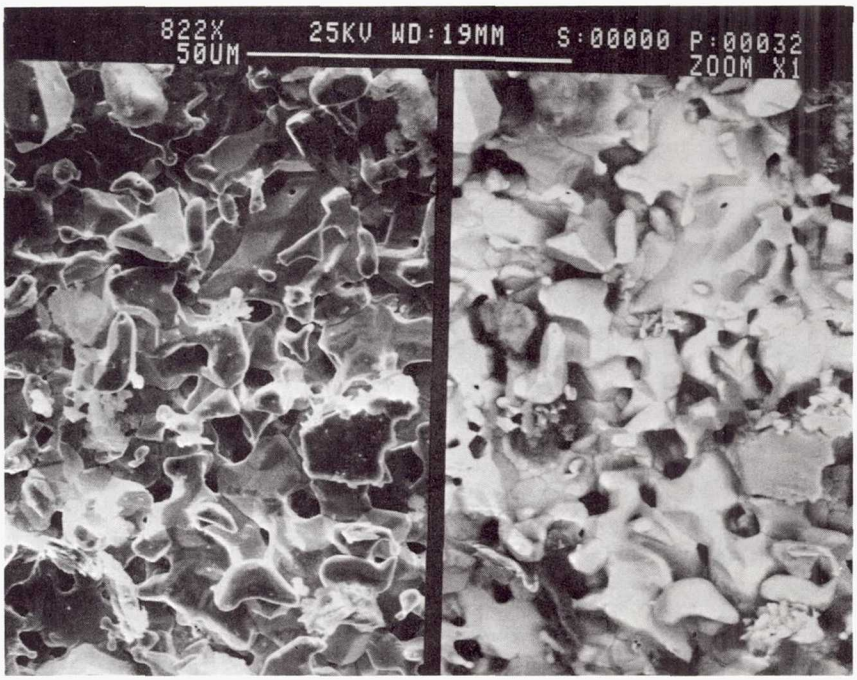

Figure 27. Surface of the downstream end of cathode WT-II insert.

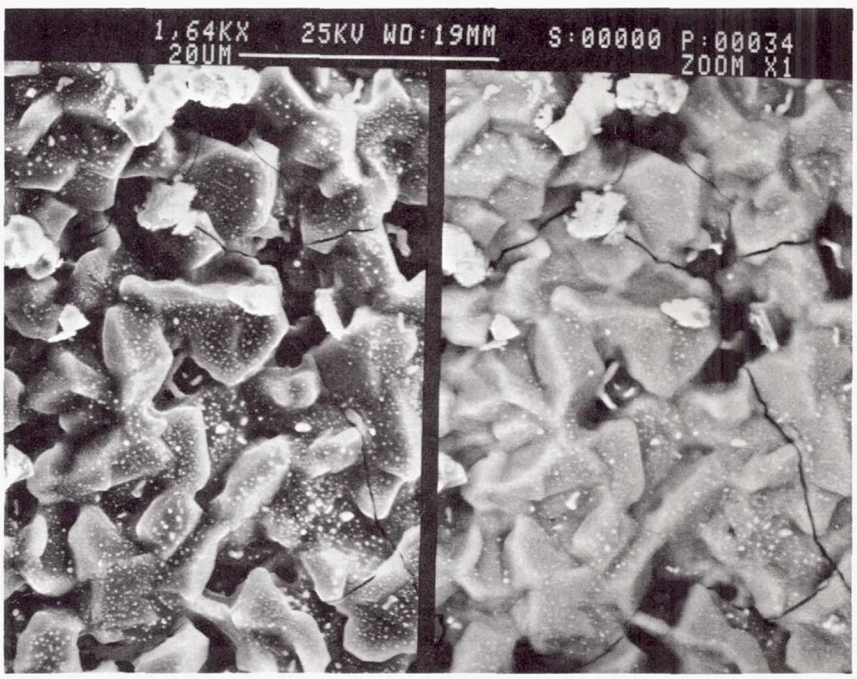

Figure 28. Second region on the insert surface of cathode WT-II.

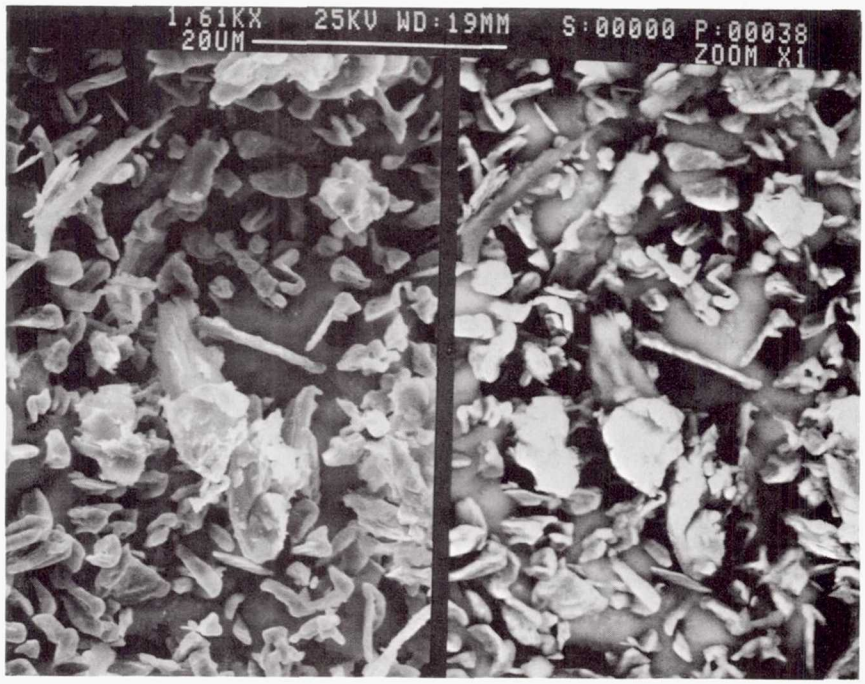

Figure 29. Surface of the upstream end of the cathode WT-II insert.

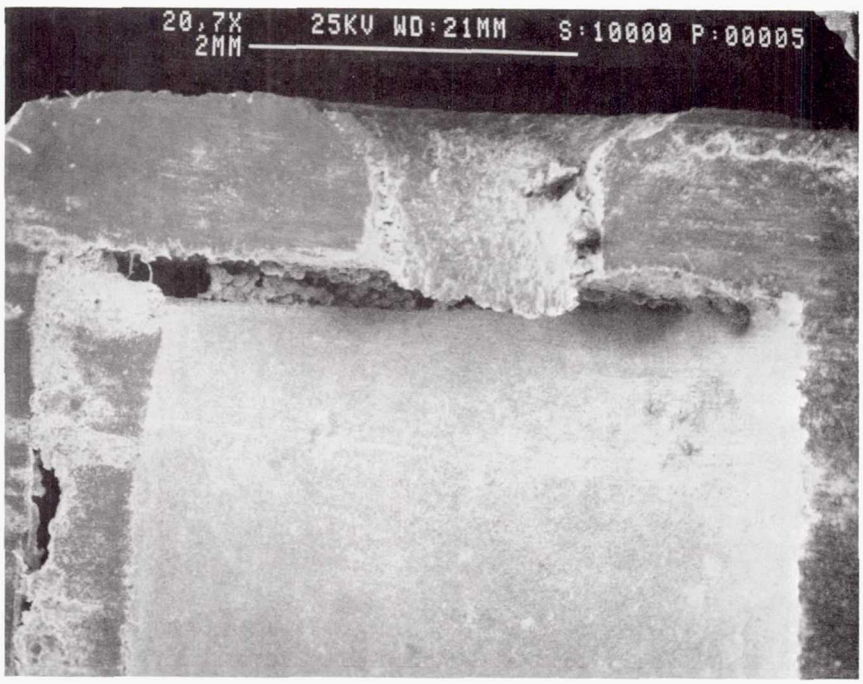

Figure 30. SE image of the orifice and downstream end of the insert of cathode TL-I. Propellant flowed from bottom to top.

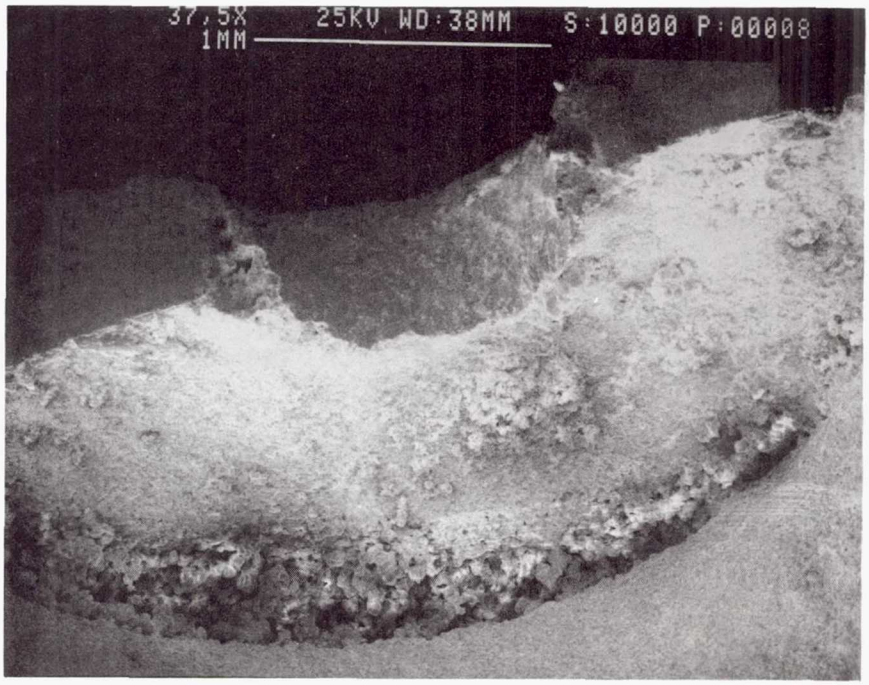

Figure 31. SE image of the inner surface of the cathode TL-I orifice plate. Propellant flowed from bottom to top.

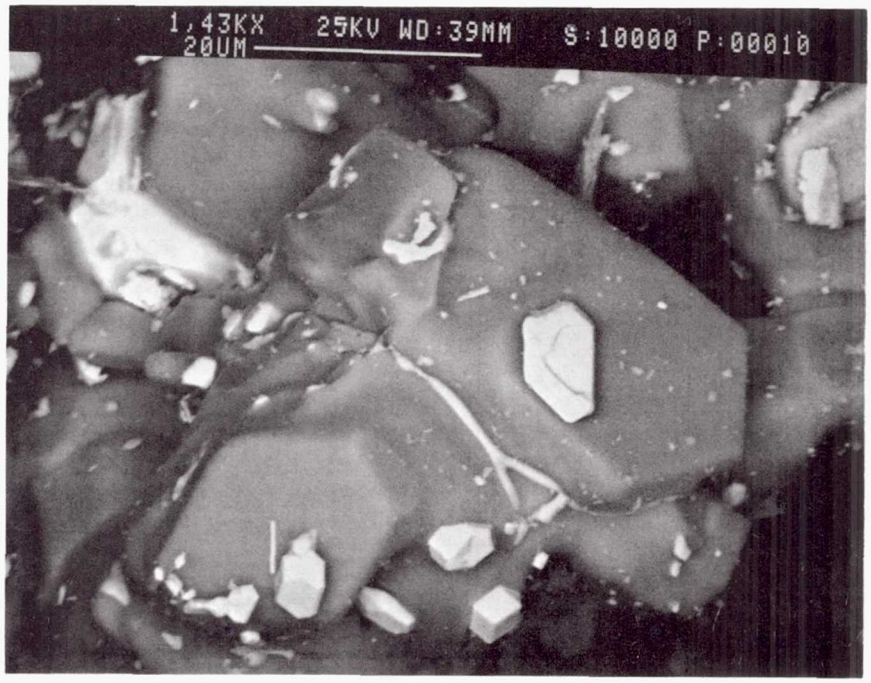

Figure 32. BSE image of coating composed of barium, aluminum, tungsten, and oxygen on the orifice plate in cathode TL-I.

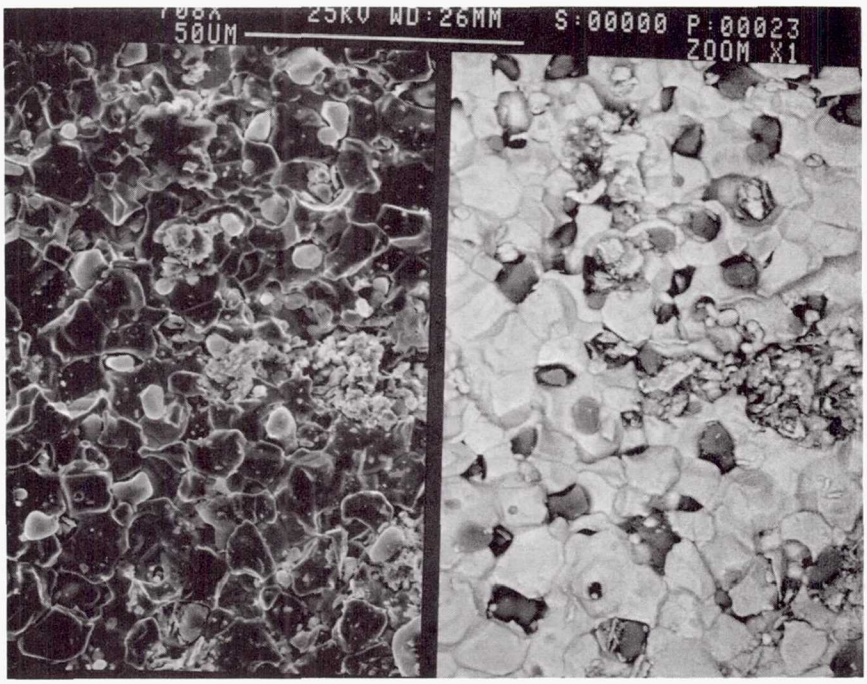

Figure 33. Surface in the first region of insert surface in cathode TL-I.

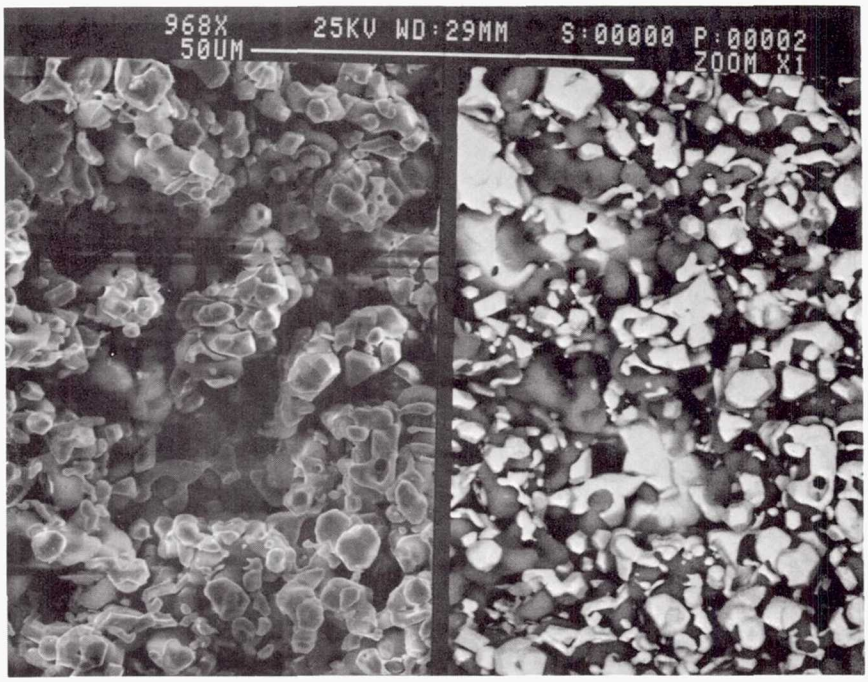

Figure 34. Surface of the second region on cathode TL-I insert.

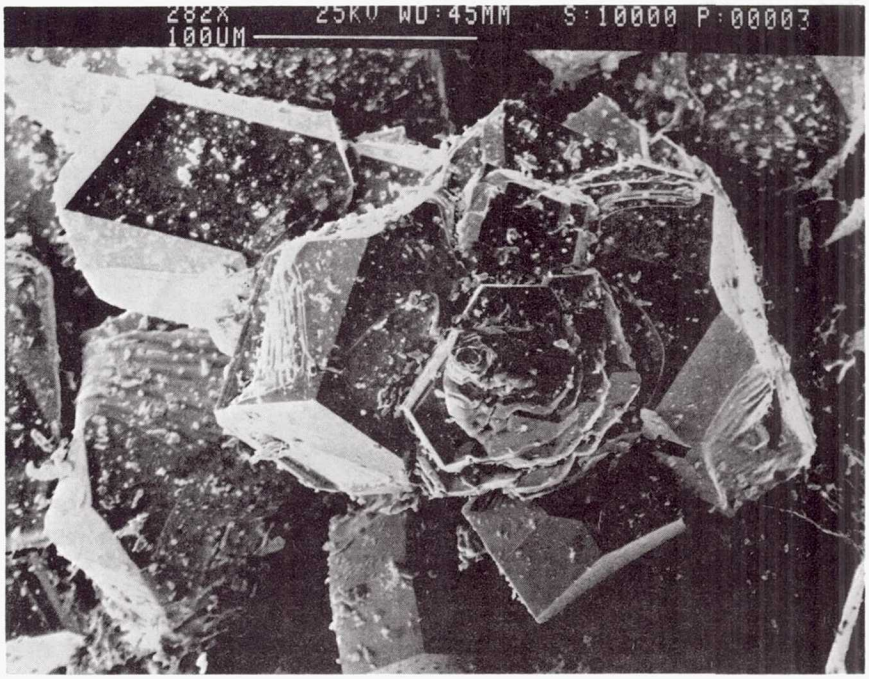

Figure 35. SE image of deposited material obtained from cathode **TL-I during** slicing.

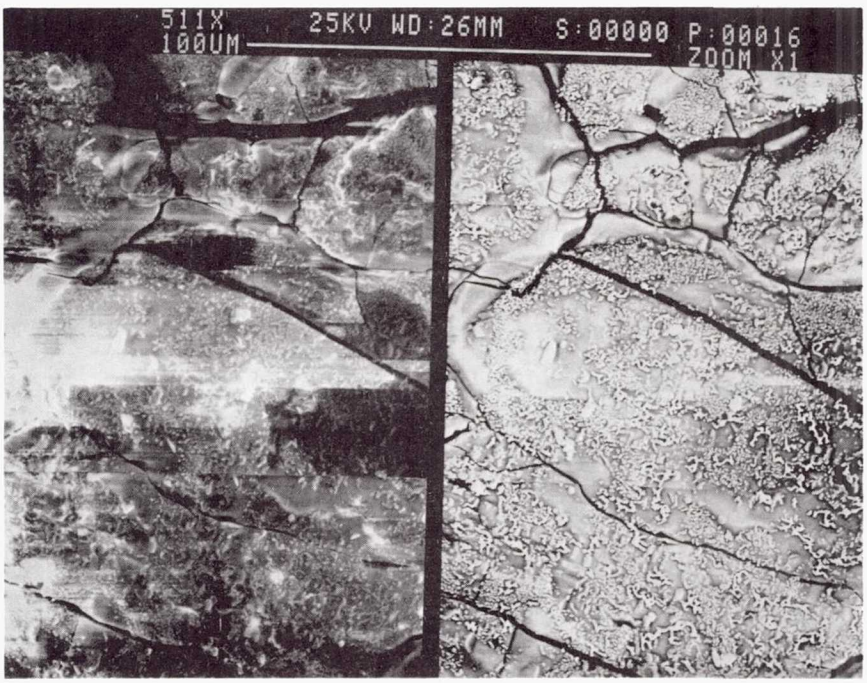

Figure 36. Surface of third region of the cathode TL-I insert.

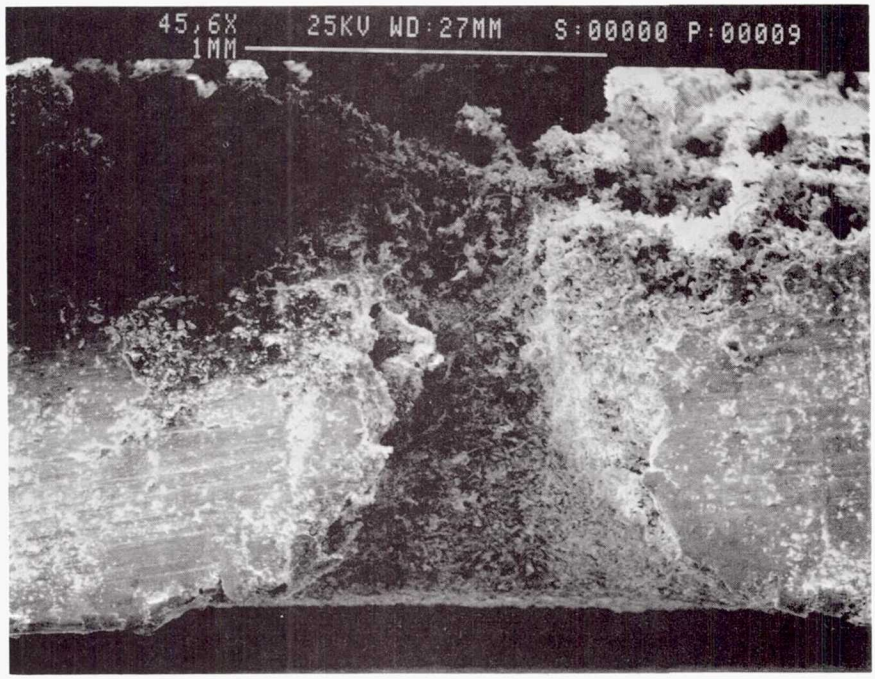

Figure 37. SE image of the orifice region of cathode TL-II. Propellant flowed from top to bottom.

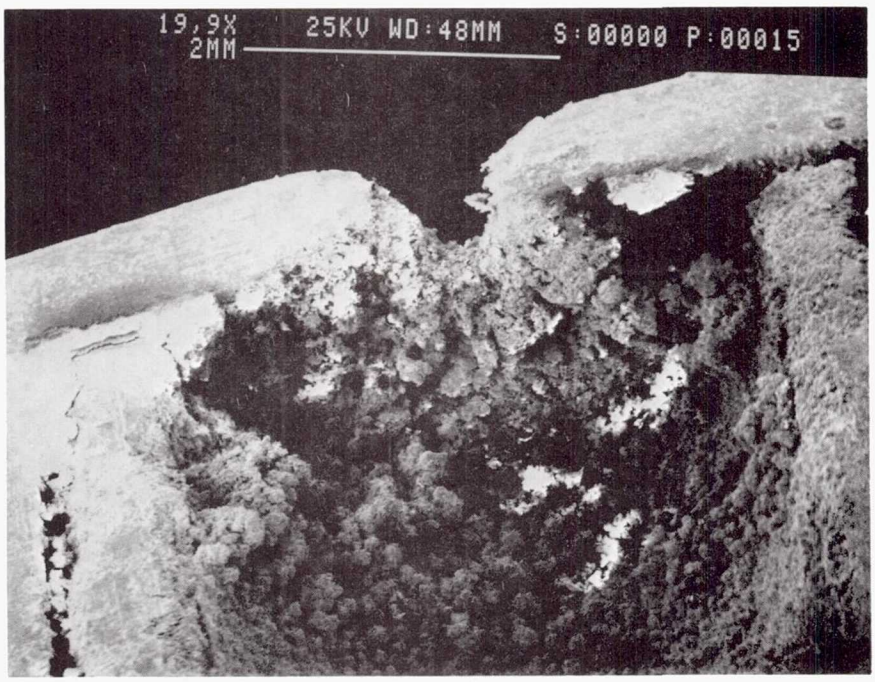

Figure 38. SE image of inner surface of the cathode TL-II orifice plate. Propellant flowed bottom to top.

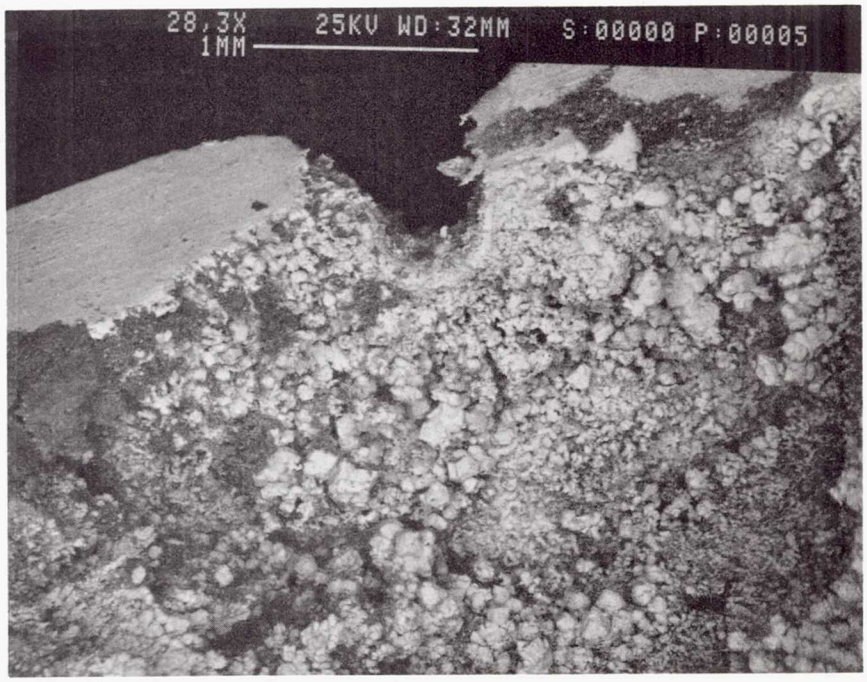

Figure 39. BSE image of inner surface of the cathode TL-II orifice plate. Propellant flowed bottom to top.

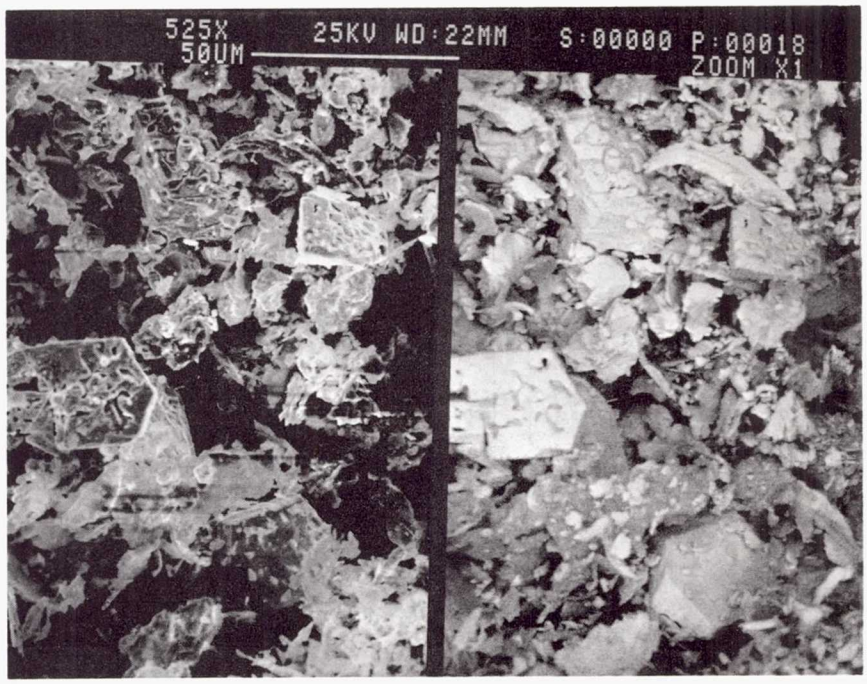

Figure 40. Surface of first region of cathode TL-II insert.

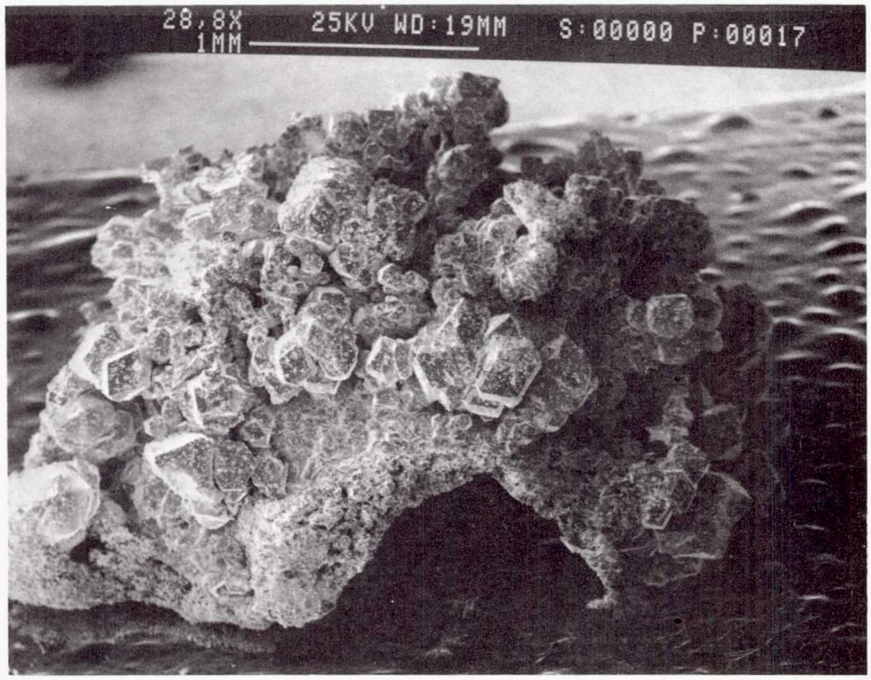

Figure 41. SE image of tungsten plug from cathode TL-II.

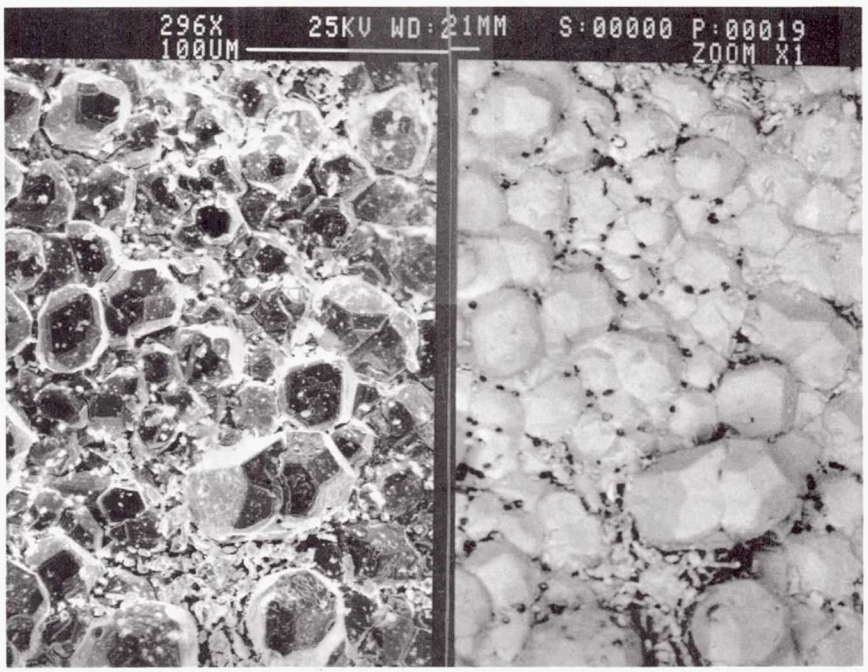

Figure 42. Surface of second region of the cathode TL-II insert.

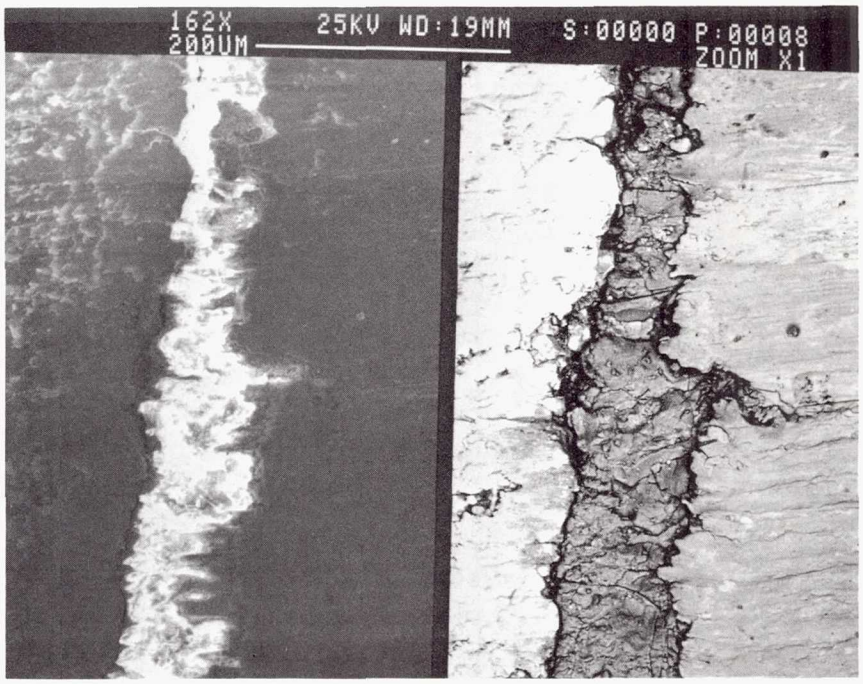

Figure 43. Gap material found between insert and cathode body tube walls in cathode TL-II.

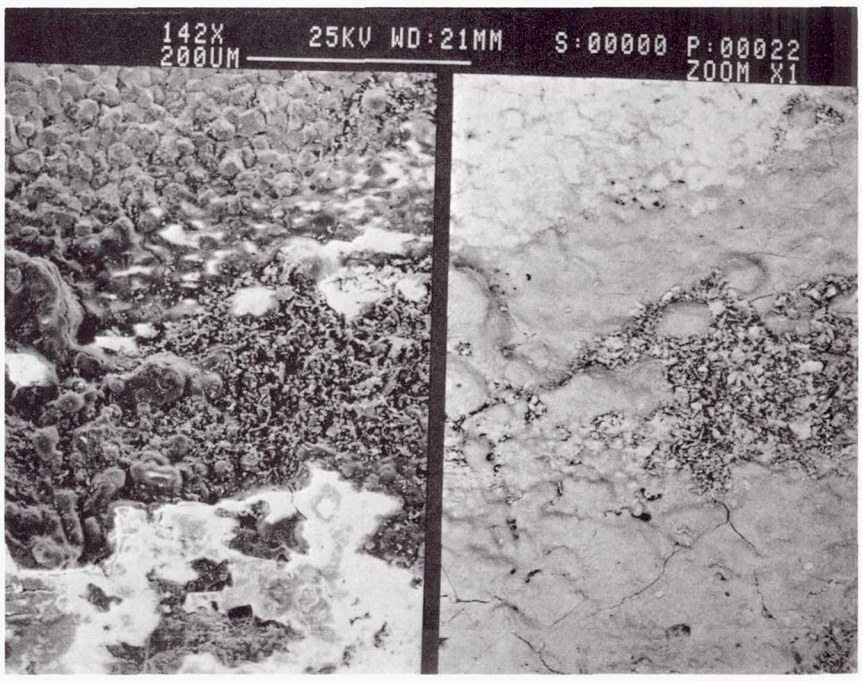

Figure 44. Surface of third region of the cathode TL-II insert.

NASA
National Aeronautics and Space Administration

Report Documentation Page

1. Report No.	2. Government Accession No.	3. Recipient's Catalog No.
NASA TM-104532 AIAA-91-2123		

4. Title and Subtitle
Microanalysis of Extended-Test Xenon Hollow Cathodes

5. Report Date

6. Performing Organization Code

7. Author(s)
Timothy R. Verhey and Michael J. Patterson

8. Performing Organization Report No.
E-6408

10. Work Unit No.
506-42-31

9. Performing Organization Name and Address
National Aeronautics and Space Administration
Lewis Research Center
Cleveland, Ohio 44135-3191

11. Contract or Grant No.

13. Type of Report and Period Covered
Technical Memorandum

12. Sponsoring Agency Name and Address
National Aeronautics and Space Administration
Washington, D.C. 20546-0001

14. Sponsoring Agency Code

15. *Supplementary Notes*
Prepared for the 27th Joint Propulsion Conference cosponsored by AIAA, SAE, ASME, and ASEE, Sacramento, California, June 24-27, 1991. Timothy R. Verhey, Sverdrup Technology, Inc., Lewis Research Center Group, 2001 Aerospace Parkway, Brook Park, Ohio 44142; Michael J. Patterson, NASA Lewis Research Center. Responsible person, Timothy R. Verhey, (216) 433-8543.

16. Abstract

Four hollow cathode electron sources were analyzed via boroscopy, scanning electron microscopy, energy dispersive x-ray analysis, and x-ray diffraction analysis. These techniques were used to develop a preliminary understanding of the chemistry of the devices that arise from contamination due to inadequate feed-system integrity and improper insert activation. Two hollow cathodes were operated in an ion thruster simulator at an emission current of 23.0 A for approximately 500 hrs. The two tests differed in propellant-feed systems, discharge power supplies, and activation procedures. Tungsten deposition and barium tungstate formation on the internal cathode surfaces occurred during the first test, which were believed to result from oxygen contamination of the propellant feed-system. Consequently, the test facility was upgraded to reduce contamination and the test was repeated. The second hollow cathode was found to have experienced significantly less tungsten deposition. A second pair of cathodes examined were the discharge and the neutralizer hollow cathodes used in a life-test of a 30-cm ring-cusp ion thruster at a 5.5 kW power level. The cathodes' test history was documented and the post-test microanalyses are described. The most significant change resulting from the life-test was substantial tungsten deposition on the internal cathode surfaces, as well as removal of material from the insert surface. In addition, barium tungstate and molybdate were found on insert surfaces. As a result of the cathode examinations, procedures and approaches have been proposed for improved discharge ignition and cathode longevity.

17. Key Words (Suggested by Author(s))	18. Distribution Statement
Hollow cathodes Xenon Electric propulsion Ion thruster	Unclassified - Unlimited Subject Category 20

19. Security Classif. (of the report)	20. Security Classif. (of this page)	21. No. of pages	22. Price*
Unclassified	Unclassified	48	A03

NASA FORM 1626 OCT 86

*For sale by the National Technical Information Service, Springfield, Virginia 22161